SELECTION OF A MULTIAXIAL FATIGUE LIFE PREDICTION METHODOLOGY: A REVIEW OF EXISTING THEORIES

by

Ioannis V. PAPADOPOULOS

Joint Research Centre, Institute for Systems, Informatics and Safety,

Structural Mechanics Unit

SELECTION OF A MULTIAXIAL FATIGUE LIFE PREDICTION METHODOLOGY: A REVIEW OF EXISTING THEORIES

Abstract

The aim of this work is first, to provide a concise but thorough assessment of some commonly used high-cycle fatigue criteria and second, to check their predictive capabilities against synchronous sinusoidal *out-of-phase* bending and torsion experimental results (i.e. sinusoidal stress signals of the same frequency but with a phase difference). This bending-torsion stress system does not closely represent real load conditions undergone by a machine part. However, it is complex enough to differentiate the various fatigue criteria and to permit a first classification of the approaches examined, according to the accuracy of their predictions.

The presentation of the various fatigue theories is preceded by a careful examination of the commonly used definitions of the stress quantities arising in the various fatigue limit criteria. Somewhat surprisingly it is observed that the very basic problems of the evaluation of the amplitude and mean value of the shear stress acting on a material plane, as well as, the calculation of the same quantities of the square root of the second invariant of the stress deviator, are still not resolved satisfactorily for non-proportional loading conditions. In the present work new definitions of these stress quantities are formulated. It is shown that these new definition are free from any inconsistency. Furthermore, these consistent definitions are used in the application of the various fatigue limit criteria in out-of-phase bending and torsion.

Poor agreement is observed between predictions and experimental results for all the criteria examined here. It ensues from the present investigation that the elaboration of a new rational high-cycle fatigue theory for metals is of prime necessity in order to comply with the ambitious objectives of the FADIN project. The basis of such a theory is presented in PART II of the present report.

INTRODUCTION

Experience acquired from single stress component high-cycle fatigue testing, has shown that many metals possess a fatigue limit. Tension-compression and rotating bending tests, are examples of single stress component loading. If the unique stress component induced by such a load fluctuates with a constant amplitude inside the stress bounds defined by the corresponding fatigue limit, then the specimen can sustain a very high number (theoretically infinite) of load cycles, without the development of a fatigue crack. To generalize the fatigue limit concept in multiaxial stress conditions the point of view commonly adopted is that there exists a *fatigue limit criterion* in terms of the periodically varying stress components. Thus the aspects of micro-damage or even short-crack propagation are not considered. The problem is then stated as follows: Given some simple fatigue information, such as experimentally established fatigue limits for single stress components, construct fatigue limit criteria for multiaxial cyclic states of stress. This generalisation of the fatigue limit concept in multiaxial stress conditions invokes the idea of the separation of the whole stress space into two parts, the unsafe and the safe one. The safe part of the stress space contains the origin and is bounded by a closed surface. Therefore, the fatigue criterion can be expressed as an inequality. Satisfaction of this inequality implies that the stress state induced by the external cyclic load, remains within the safe part of the stress space. Employing this concept various authors have proposed many fatigue criteria over decades of research. In spite of the high number of proposals, there is not yet a universally accepted approach. For the older criteria this is due, at least partly, to the fact that these common criteria are initially conceived for in-phase cyclic stress systems (i.e. proportional cyclic loading). In principle, as we see later, these criteria can be extended to cover out-of-phase load conditions. More recent proposals discuss specifically the problem of out-of-phase cyclic loading. The main objective of the present work is to investigate the appropriateness of several fatigue criteria.

Because of the high number of the fatigue theories examined, it is found useful to give first a complete set of the stress quantities arising in the various criteria. Then, the different criteria are classified into three categories namely, critical plane approaches, approaches based on the stress invariants and approaches using averages of stress quantities within an elementary material volume. Not all the existing criteria have been included in this study, simply because such an enterprise would be too lengthy. An rather complete list of existing fatigue criteria can be found for instance, in Papadopoulos [1]. The choice of the theories presented here, is therefore somewhat arbitrary. In general, more attention has been attributed to recent proposals. Concerning older theories, care has been taken to include those approaches, that the author feels to be among the more widely used in high-cycle fatigue. The predictions of these criteria against out-of-phase bending and torsion experimental results, collected from the relevant literature, are used as a decisive test, to draw some conclusions. However, not all the examined criteria are controlled against the available test data. The reasons of excluding of this evaluation process some of the criteria presented, are duly explained where appropriate.

DEFINITION OF SOME USEFUL STRESS QUANTITIES

Stress quantities related to a material plane

Normal Stress

Let us consider a material point of a body submitted to cyclic loading, *(Figure 1)*. Let us consider further a material plane, denoted as Δ, passing through the point under consideration. A plane is located by its unit normal vector $\underset{\sim}{n}$. This unit vector in turn is described by its spherical angles (φ,θ), *(Figure 1)*. On the plane Δ is acting the stress vector, denoted as $\underset{\sim}{S}_n$, given by:

$$\underset{\sim}{S}_n = \underset{\sim}{\Sigma} \cdot \underset{\sim}{n} \tag{1}$$

The stress vector $\underset{\sim}{S}_n$ is decomposed into two vectors, one perpendicular to the plane Δ, which is the normal stress vector $\underset{\sim}{N}$ and one tangential to Δ, which is the shear stress vector $\underset{\sim}{C}$. The normal stress $\underset{\sim}{N}$, carried out by the unit vector $\underset{\sim}{n}$, is precisely the projection of $\underset{\sim}{S}_n$ on $\underset{\sim}{n}$, *(Figure 1)*:

$$\underset{\sim}{N} = (\underset{\sim}{n} \cdot \underset{\sim}{S}_n)\underset{\sim}{n} \Rightarrow \underset{\sim}{N} = (\underset{\sim}{n} \cdot \underset{\sim}{\Sigma} \cdot \underset{\sim}{n})\underset{\sim}{n} \tag{2}$$

The shear stress vector $\underset{\sim}{C}$, is equal to the difference of these two vectors:

$$\underset{\sim}{C} = \underset{\sim}{S}_n - \underset{\sim}{N} \Rightarrow \underset{\sim}{C} = \underset{\sim}{\Sigma} \cdot \underset{\sim}{n} - (\underset{\sim}{n} \cdot \underset{\sim}{\Sigma} \cdot \underset{\sim}{n})\underset{\sim}{n} \tag{3}$$

The above definition means that the shear stress vector $\underset{\sim}{C}$ is the orthogonal projection of the stress vector $\underset{\sim}{S}_n$ onto the plan Δ, *(Figure 1)*.

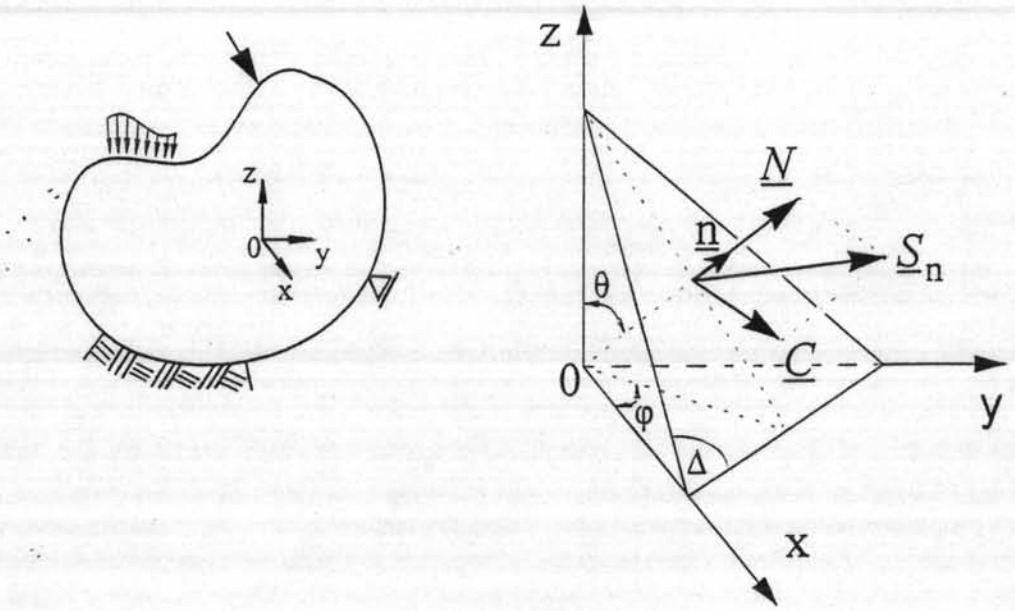

Figure 1 .Stress vector $\underset{\sim}{S}_n$, normal stress vector $\underset{\sim}{N}$ and shear stress vector $\underset{\sim}{C}$, acting on a material plane Δ

During a complex cyclic loading the tip of the stress vector S_n describes a closed space curve Ψ, (*Figure 2*). Clearly, the normal stress N conserves its direction invariant. The tip of the vector N oscillates between two points on the line defined by n, these two points being the extremes of the projection of the curve Ψ onto n. Therefore, during a cycle of a complex periodic load the vector N acting on Δ changes in magnitude but not in direction. Because of this fact the definition of the amplitude and mean value of the normal stress N can be based on the study of its algebraic value $(n \cdot \Sigma \cdot n)$ alone, which in turn is a scalar periodic function of time. Finding the amplitude and mean value of a scalar periodic function is a trivial problem. Indeed, the semi-difference between the maximum and minimum values of the function provides its amplitude, whereas the semi-sum yields its mean value. :

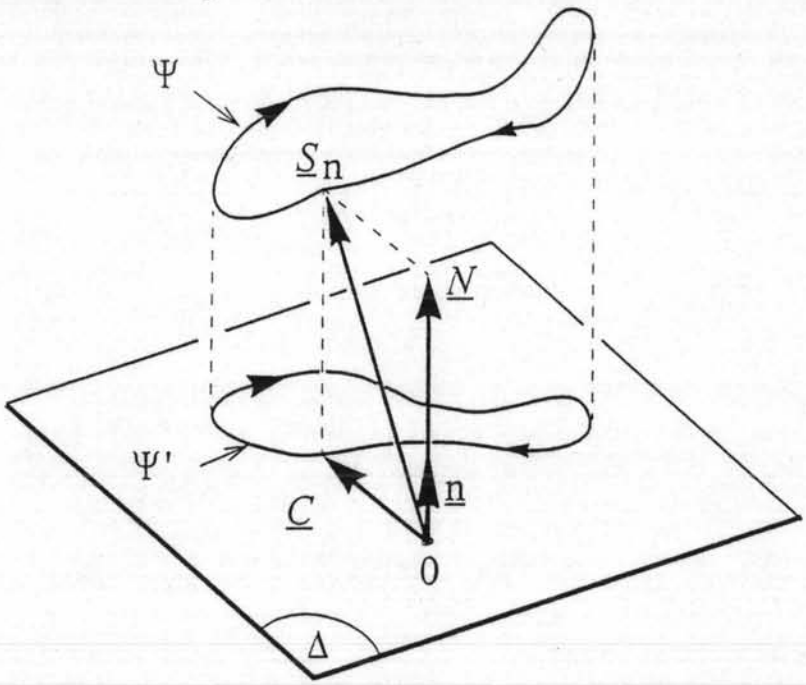

Figure 2 .Evolution of stress quantities acting on a material plane Δ, during a complex cyclic loading

Therefore, the amplitude of the normal stress is defined to be equal to the semi-difference between the maximum and minimum values that $(n \cdot \Sigma \cdot n)$ achieves inside a load period P, whereas the corresponding mean value is equal to their semi-sum

$$N_a = \frac{1}{2}\left\{ \max_{t \in P} (n \cdot \Sigma(t) \cdot n) - \min_{t \in P} (n \cdot \Sigma(t) \cdot n) \right\}$$
$$N_m = \frac{1}{2}\left\{ \max_{t \in P} (n \cdot \Sigma(t) \cdot n) + \min_{t \in P} (n \cdot \Sigma(t) \cdot n) \right\} \quad (4)$$

Clearly, the maximum value of the normal stress is equal to:

$$N_{max} = N_a + N_m \quad (5)$$

Shear Stress

The situation is much more complex regarding the definition of the amplitude and mean value of the shear stress. The complexities arise from the fact that, unlike the normal stress vector N which conserves its direction, the shear stress vector C changes in *magnitude and direction* inside each load cycle. Indeed, during a load cycle the tip of the shear stress vector C describes on Δ a closed curve Ψ', which in fact is the projection on Δ of the space curve Ψ described by the tip of the stress vector S_n, (*Figure 2*). In conclusion, C is a vectorial periodic function of time. Therefore, we face the problem of finding the amplitude and mean value of a vectorial function and this is not a trivial problem. However, let us assume that by some means we have succeeded in finding the amplitude C_a of the shear stress acting on a arbitrarily chosen plane Δ. Of course, the curve Ψ' described by C is different on different planes passing through the point under consideration. Therefore, the shear stress amplitude C_a depends on the orientation of the plane on which it acts, that is it is a function of n or equivalently a function of φ and θ, i.e. $C_a(\varphi,\theta)$. To find the maximum shear stress amplitude $_{a,max}$ one has to take into account all the planes passing through the point under consideration. This can be done by searching the maximum of $C_a(\varphi,\theta)$ over the angles φ and θ:

$$C_{a,max} = \max_{\varphi,\theta} \left\{ C_a(\varphi,\theta) \right\} \tag{6}$$

Let us denote by (φ^*,θ^*) the pair of φ and θ that provides the solution of the maximisation problem above. Clearly this couple (φ^*,θ^*) defines the critical plane. Let us turn now our attention to the most critical problem left unsolved, that is the evaluation of C_a on a given material plane Δ.

Review of previous work

To the author's best knowledge two proposals have been formulated in the past for the general solution of the problem of finding C_a and C_m. The first one seems to be first discussed by Crubisic and Simbürger [2]. Although the fatigue criterion proposed by these authors is not of the critical plane type, the evaluation of the amplitude and mean value of the shear stress acting on a material plane Δ, is a necessary intermediate step in their approach. To define the shear stress amplitude they imagine all the lines lying on Δ passing from the origin O and they project the curve Ψ' on all these lines. The shear stress amplitude is defined to be equal to half the length of the longest among these projections of Ψ'. Therefore, this method will be called the *Longest Projection* proposal to reflect the above definition of shear stress amplitude. Let us denote as $A'Z'$ this longest projection; then one has $C_a = A'Z'/2$, (*Figure 3*). The mean value of the shear stress is given by the segment OM', where M' is the midpoint of the longest projection $A'Z'$ of Ψ', i.e. $C_m = OM'$ see (*Figure 3*).

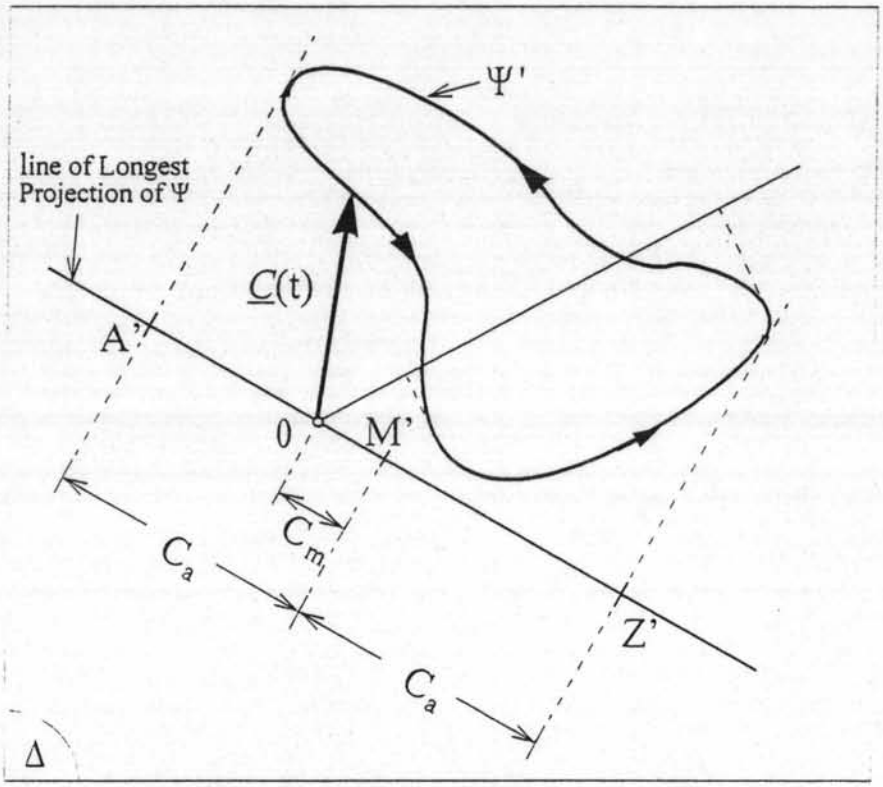

Figure 3 . The Longest Projection proposal

In what follows, it is presented a counter-example, that is an example of a particular shear stress path for which the Longest Projection proposal falls short. To this end let us assume that the tip of the shear stress vector C describes on plane Δ a path $A \rightarrow Z \rightarrow A$, which indeed is a linear segment AZ. The segment AZ is located such that the radius OM joining the origin with its midpoint is perpendicular to AZ, (*Figure 4*).

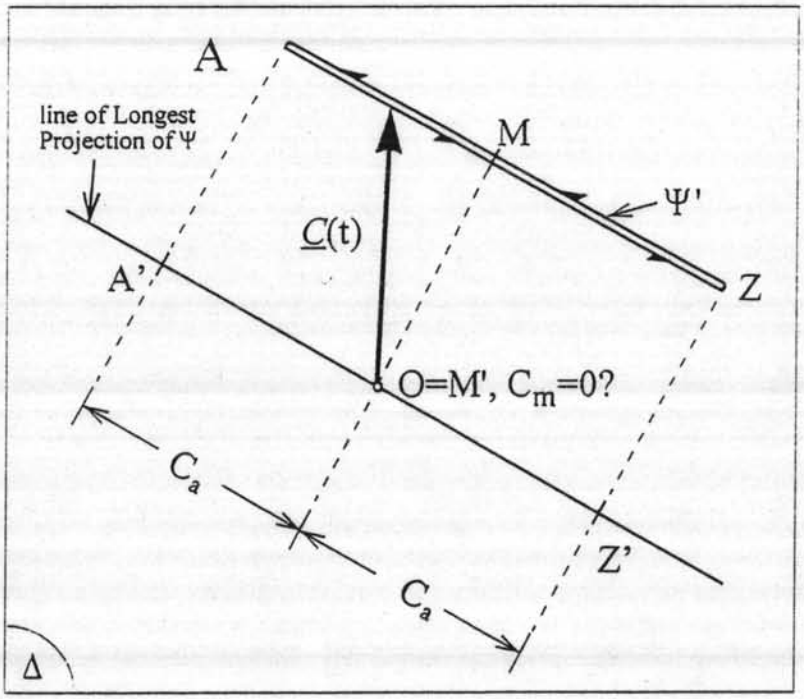

Figure 4 .Counter-example inducing in breakdown the Longest Projection proposal

Intuitively, one concludes that the shear stress amplitude is equal to half the length of AZ, i.e. $C_a = AZ/2$, whereas the mean shear stress is equal to the length of the segment OM joining the origin with the midpoint of AZ, i.e. $C_m = OM$, (*Figure 4*). Let us apply the Longest Projection proposal in this case. According to this, one seeks to find the line passing from O, onto which the projection of AZ becomes maximum. Clearly, this line is parallel to AZ, (*Figure 4*). The projection of AZ on this line, denoted as $A'Z'$, is obviously equal to AZ itself. The shear stress amplitude according to the Longest Projection proposal is equal to $C_a = A'Z'/2$. This in turn is equal to the intuitively found value of $C_a = AZ/2$, because of the equality $AZ = A'Z'$. However, the midpoint M' of the projection $A'Z'$ coincides with the origin O indicating that in this case, according to the Longest Projection proposal, the mean shear stress is zero, i.e. $C_m = 0$, (*Figure 4*). This result seems to be wrong and at least against our intuition, which provided the (correct) value of $C_m = OM$. The counter-example studied here is just one example where the Longest Projection proposal breaks down. One can find many other situations where this proposal leads to ambiguous results.

The second proposal for solving the problem under consideration is based on the concept of the longest chord of the curve Ψ'. It will be called precisely the *Longest Chord* proposal. This method has been discussed in some detail in Lemaitre and Chaboche, [3]. According to this approach one must consider all the chords joining any two points of the curve Ψ' and find among them the chord of maximum length, (*Figure 5*). The amplitude of the shear stress acting on Δ is equal to half the length of the longest chord, denote as AZ, of the curve Ψ', (*Figure 5*). Then one has $C_a = AZ/2$. The value of the mean shear stress according to the Longest Chord proposal is equal to the length of the segment that joints the origin O with the midpoint M of AZ, (*Figure 5*).

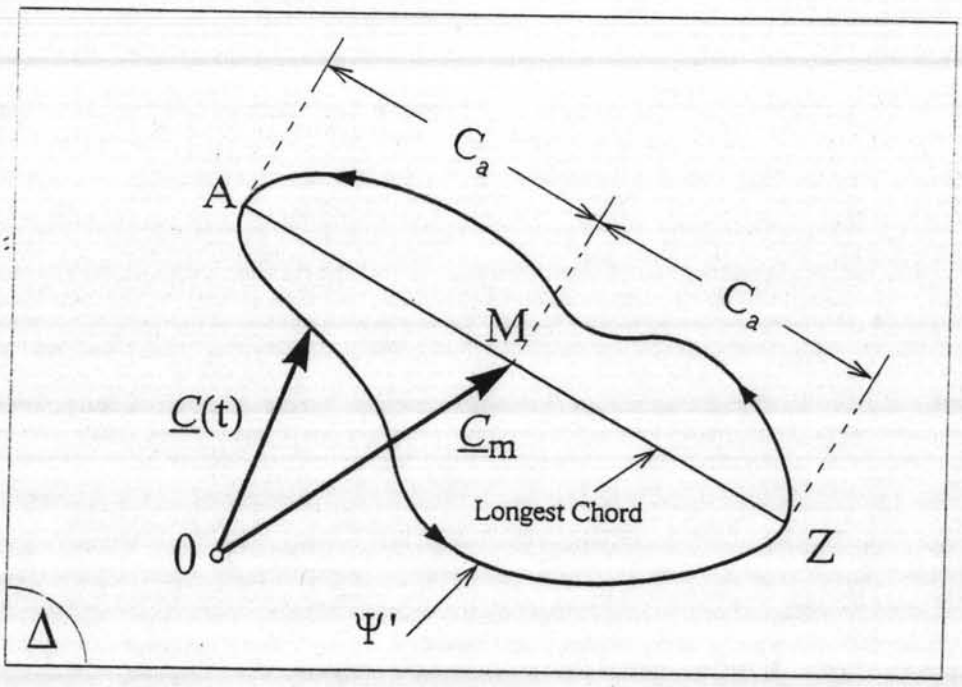

Figure 5 .The Longest Chord proposal

If one applies this method to the Longest Projection counter-example of *(Figure 4)* described before, the correct values $C_a = AZ/2$ and $C_m = OM$ will result. Undoubtedly, the Longest Chord proposal constitutes a progress with respect to the Longest Projection method. However, there are situations where this approach breaks down as well. Again, the problems arise from the evaluation of the mean shear stress. This is defined above to be equal to the length of the segment that joints the origin O to the midpoint of the longest chord of Ψ'. But one can easily conceive that the longest chord of a curve is not necessarily unique. For instance, let us assume that the curve Ψ' described by $\underline{C}$ on a given plane Δ is an isosceles triangle ABC, *(Figure 6)*.

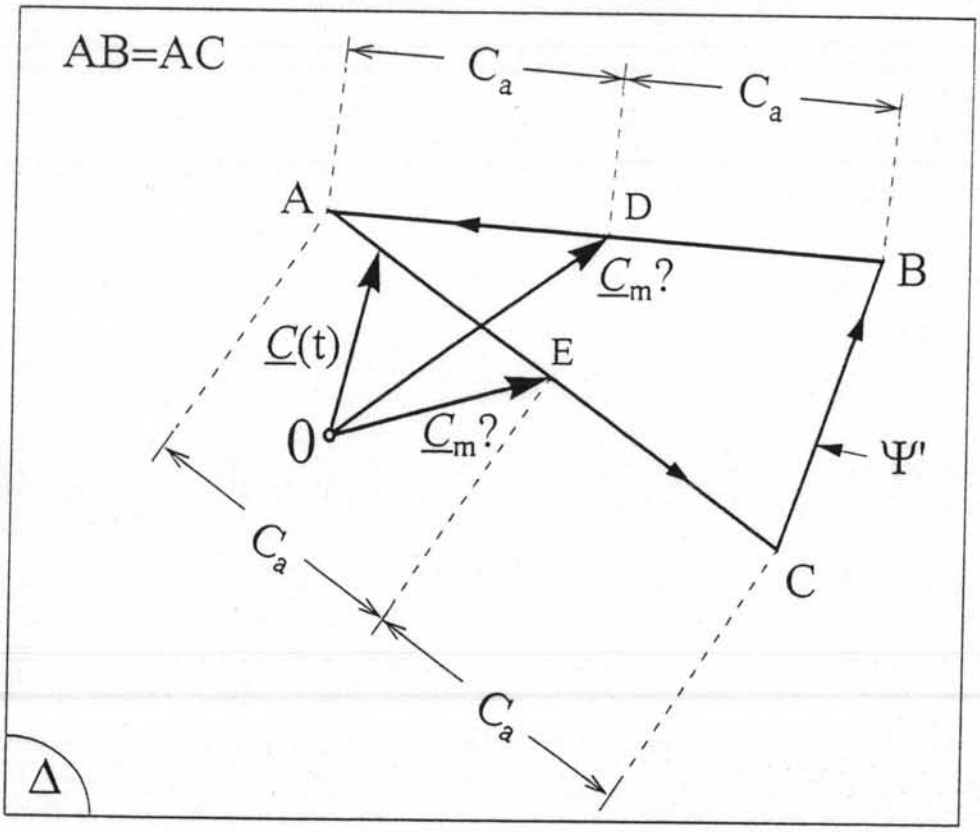

Figure 6 .Counter-example for which the Longest Chord proposal falls short

Then we have two equal longest chords, i.e. AB and AC. Although this does not affect the value of C_a, which is given by $C_a = AB/2 = AC/2$, the mean shear stress is not uniquely defined any more. If D et E are the midpoints of AB and AC, *(Figure 6)*, which one of the segments OD or OE has to be used to calculate a mean shear stress value C_m? This example is used as a counter-example illustrating a situation where the Longest Chord proposal falls short. One can find many other loading conditions for which uniqueness of the calculated shear stress values is not ensured. In conclusion, the counter-examples, *(Figure 4)* and *(Figure 6)*, even if not of immediate practical interest, served to underline the need for a new definition of C_a and C_m, which must be free from the inconsistencies encountered with the methods examined before.

A proposal based on the concept of the minimum circumscribed circle

As it has seen, the tip of the vector C describes on Δ a possibly complicated closed curve Ψ'. To define unambiguously the shear stress amplitude, the author came to the conclusion that this amplitude must be conceived as the maximum excursion of the tip of the shear stress vector C from a mean shear stress state described by a fixed vector $\underset{\sim}{C}_m$ on Δ. Therefore, unlike the previous proposals that started by researching first the amplitude and subsequently the mean shear stress, here we seek to determine first the mean shear stress state. Let us assume that by some means such a mean shear stress vector $\underset{\sim}{C}_m$ has been located on Δ. Then the amplitude of the shear stress is equal to the length of the segment that joints the tip of the vector $\underset{\sim}{C}_m$ to the most distant point on the curve Ψ'. The main problem is then the procedure that permits to locate $\underset{\sim}{C}_m$. Here, it is proposed to take as $\underset{\sim}{C}_m$ the vector that points to the centre of the minimum circumscribed circle to the curve Ψ'. The shear stress amplitude on the plane Δ is then obviously equal to the radius of this circle. The present approach is called precisely the *Minimum Circumscribed Circle* proposal. The idea of the minimum circumscribed circle has first been put forward by Dang Van in [4], but an improper mathematical formulation of the problem was presented in that paper.

In the following the correct mathematical formulation of the problem of finding the minimum circumscribed circle to a plane curve is established. The formulation presented here was first elaborated in [5]. To make things clear let us consider a plane Δ defined by its unit normal vector n. On this plane we compute the shear stress C, Equation (3), at a finite number of instants t_i, i=1,2...m of the load period. Thus the set $C(t_i)$, i=1,2...m is formed. This means that the curve Ψ' described by C on Δ is approximated by a polygon P of m vertices. By increasing the number m one can make the polygon P to be as close to Ψ' as he wishes. Therefore, in what follows the problem of searching the minimum circumscribed circle to polygon P will be pursued. The m vertices of P are indeed described by the set of vectors $C(t_i)$, i=1,2...m. There are infinitely many circles that can be drawn on Δ to contain at their interior the polygon P. The smallest one of these circles is what we have called the *minimum circumscribed circle* to P. The minimum circumscribed circle to a plane polygon is unique, [6]. The centre of this circle determines the mean shear stress $\underset{\sim}{C}_m$ on the plane Δ. Mathematically the problem of finding $\underset{\sim}{C}_m$ is formulated as follows:

$$\underset{\sim}{C}_m = \min_{\underset{\sim}{w}} \left\{ \max_{t_i} \left\| \underset{\sim}{C}(t_i) - \underset{\sim}{w} \right\| \right\} \tag{7}$$

where $C(t_i)$ is an element of the set of the m vertices of P and w a point of plane Δ. The way that the min-max problem, Equation (7), has been built needs explanation, (*Figure 7*).

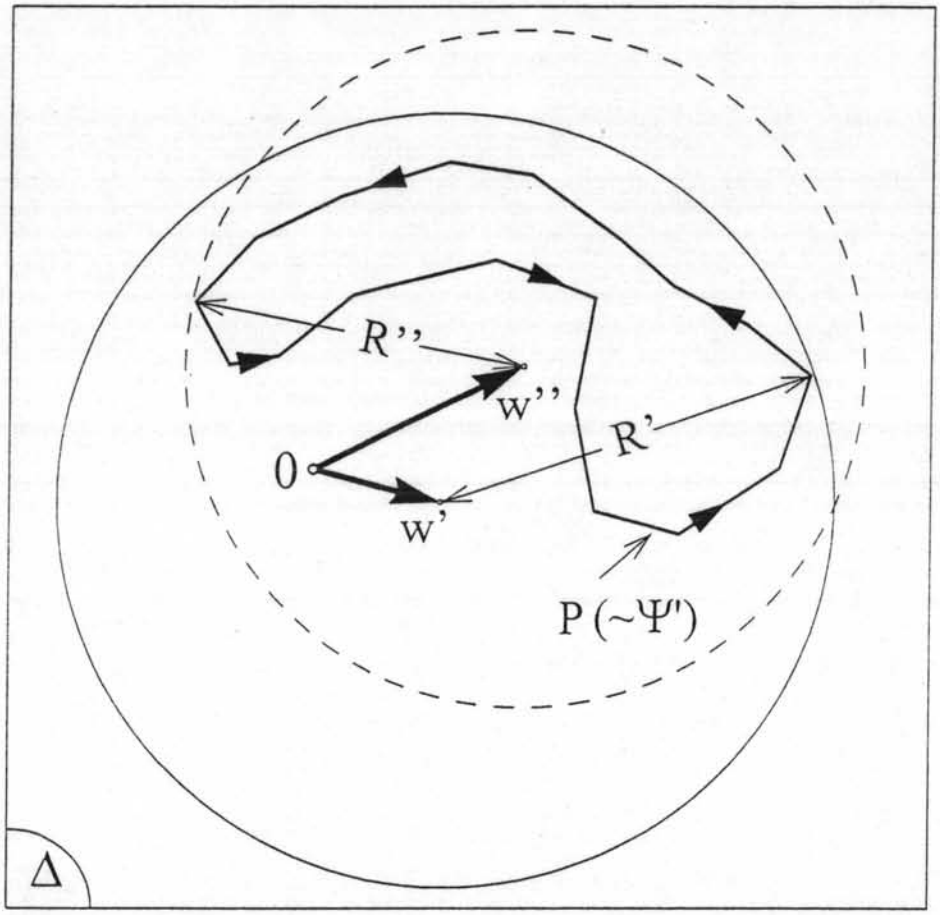

Figure 7 .Formulating the min-max problem for the research of the Minimum Circumscribed Circle

To illustrate that, let us assume that one chooses arbitrarily a point w' on Δ, as a candidate for being the centre of the minimum circumscribed circle to $\tilde{P}$, (*Figure 7)*. Even after a candidate centre has been chosen, the number of circles drawn with w' as centre and containing the polygon P, is still infinite. However, among these infinitely many circles there is a smallest one. Its radius is equal to the longest line segment, among the m in number line segments joining w' with the vertices of P, (*Figure 7)*. Therefore, for a given w' the radius R' of the smallest circle centred on w' and circumscribing P is equal to:

$$R' = \max_{t_i} \left\| \underset{\sim}{C}(t_i) - \underset{\sim}{w'} \right\| \tag{8}$$

The relationship above, corresponds precisely to the maximizing part of the min-max problem, Equation (7). The minimizing part of the min-max problem can be understood as follows. After having found the smallest circumscribed circle centred on a candidate centre w', one can chose another candidate centre w'' leading to a circle always containing P, but now with a radius R'' smaller than the previously found R'

and so forth, (*Figure 7*). In other words one is seeking to minimize the quantity,

$$\left(\max_{t_i} \left\| \underset{\sim}{C}(t_i) - \underset{\sim}{w} \right\| \right)$$

by varying w and this corresponds precisely to the minimizing part of the min-max problem, Equation (7). However, the explanation of how the min-max problem has been built does not provide any indication of how this problem can be solved. The solution of the min-max problem, Equation (7), is instead based on the following theorem first established in [5] in a more general context:

Theorem

The minimum circumscribed circle to a plane polygon P is: either one of the circles drawn with diameter a line segment joining any two vertices of P, or one of the circumcircles of all the triangles generated from every three vertices of P.

The interesting reader can consult reference [5] for the demonstration of this theorem. The number of line segments defined by any two vertices of P is equal to the number of the combinations of the m vertices of P taken two at a time,

$$n_D = \binom{m}{2} \Rightarrow n_D = \frac{m!}{2!(m-2)!} \tag{9}$$

whereas the number of all triangles that can be generated combining every three vertices of P is equal to the number of combinations of m taken three at a time:

$$n_T = \binom{m}{3} \Rightarrow n_T = \frac{m!}{3!(m-3)!} \tag{10}$$

The algorithm for finding the minimum circumscribed circle to the polygon P is then straightforward:

Algorithm

- *First, the set of all the line segments formed by every two vertices of P is assembled. It is noticed that this set is composed by all the sides and all the chords of P. The number of the elements of this set is equal to n_D, Equation (9). For each line segment, which is indeed a chord or a side of P, a circle is drawn with diameter the line segment under consideration.*
- *Second, the set of all the triangles generated from every three vertices of P is built. The number of the triangles thus formed is equal to n_T, Equation (10). For every triangle its circumcircle is drawn.*

• *Third, for each circle, among the $n_D + n_T$ circles drawn in the two previous steps, a check is performed to find out if this circle contains the whole polygon P. This is done by calculating the distances from the centre of this circle to all the vertices of P. If these distances are all smaller or equal than the radius of the circle under consideration, then the circle circumscribes the polygon P. For such a circle, the co-ordinates of its centre and the length of its radius are stored in a set denoted as R.*

• *Fourth, the elements of set R are all circles that contain the polygon P. In view of the theorem announced before, the circle with the smallest radius among the elements of set R is the minimum circumscribed circle to the polygon P.*

Once the centre $\underset{\sim}{C}_m$ of the minimum circumscribed circle to the curve Ψ' (approximated by the polygon P) has been located, the mean value and the amplitude of the shear stress acting on Δ are given by:

$$C_m = \left\| \underset{\sim}{C}_m \right\| \qquad C_a = \max_{t_i} \left\| \underset{\sim}{C}(t_i) - \underset{\sim}{C}_m \right\| \tag{11}$$

It is noticed that an attempt for solving the min-max problem, Equation (7), has been done in [7]. However, the algorithm given there is an algorithm of incremental type the convergence of which to the solution is not demonstrated. (*Figure 8)* illustrates the application of the Minimum Circumscribed Circle proposal in the loading cases of the counter-examples, (*Figure 4)* and (*Figure 6)*, that induced the breakdown of the Longest Projection and Longest Chord proposals respectively.

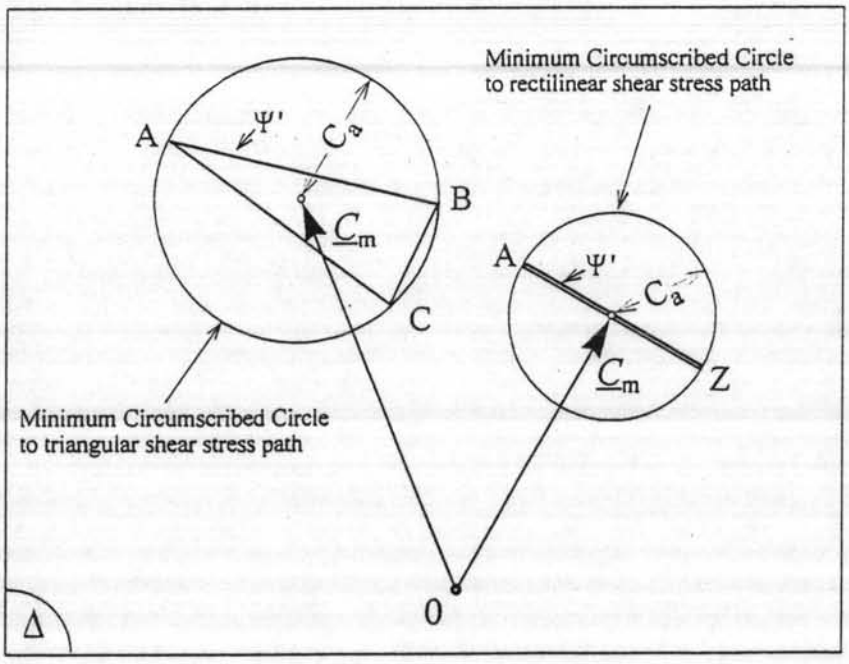

Figure 8 .Application of the Minimum Circumscribed Circle proposal in the previous examples

From (*Figure 8)* it is clear that the proposed approach leads to the correct solution in both cases. Furthermore, because of the uniqueness of the Minimum Circumscribed Circle it does not exist any counter-example inducing in inconsistent results this approach. It seems then that this proposal is a valuable method for computing the mean value C_m and amplitude C_a of the shear stress acting on a material plane Δ. Of course, to find $C_{a,max}$ all the planes passing through the point under consideration must be considered and the maximisation process described by Equation (6) has to be applied. An interesting remark is that if the curve Ψ' possesses a centre of symmetry then the centre of its minimum circumscribed circle is its centre of symmetry.This property of the centre of symmetry is fully exploited in the examples shown below.

Examples

Application in out-of-phase bending and torsion

Let us examine now how the above definitions are applied in synchronous sinusoidal out-of-phase bending and torsion. For the choice of the frame O.xyz shown in (*Figure 9)* the stress state is described by the tensor:

$$\underset{\sim}{\Sigma} = \begin{bmatrix} \Sigma_{xx} & \Sigma_{xy} & 0 \\ \Sigma_{yx} & 0 & 0 \\ 0 & 0 & 0 \end{bmatrix} \Rightarrow \underset{\sim}{\Sigma} = \begin{bmatrix} \Sigma_{xx,a}\sin\left(\frac{2\pi t}{P}\right) + \Sigma_{xx,m} & \Sigma_{xy,a}\sin\left(\frac{2\pi t}{P} - \delta\right) + \Sigma_{xy,m} & 0 \\ \Sigma_{xy,a}\sin\left(\frac{2\pi t}{P} - \delta\right) + \Sigma_{xy,m} & 0 & 0 \\ 0 & 0 & 0 \end{bmatrix} \quad (12)$$

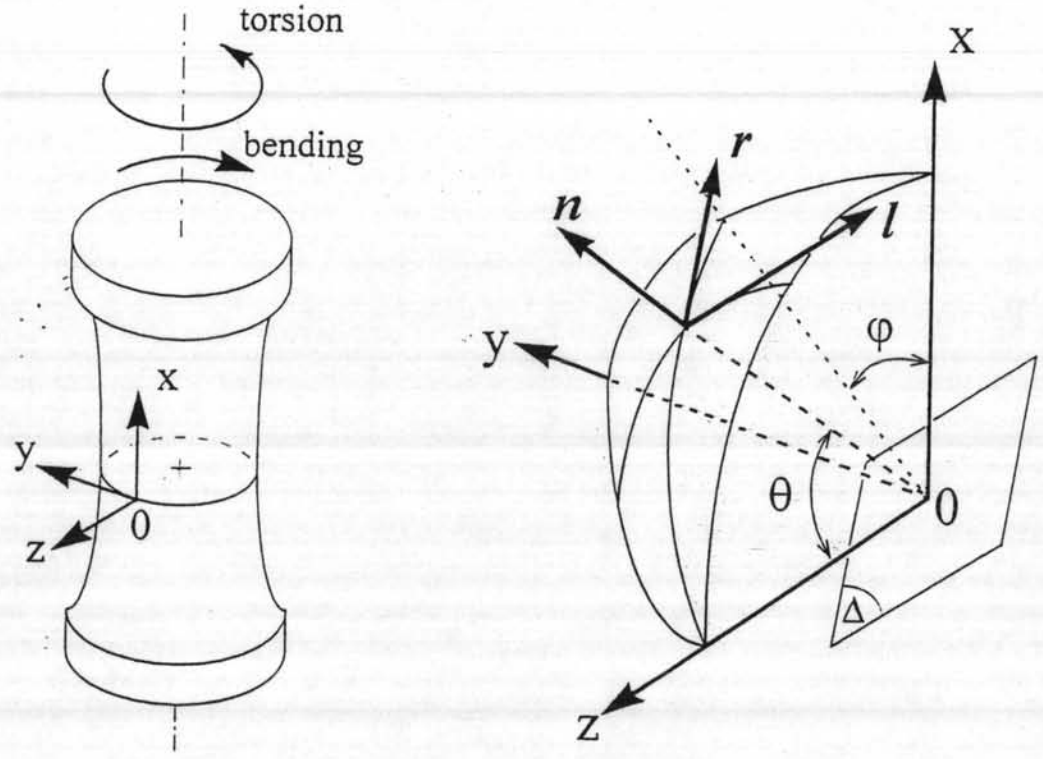

Figure 9 .O.xyz frame attached at any point of a specimen subjected to bending and torsion and O.nlr frame attached at material plane Δ.

. An elementary material plane Δ passing through O is defined by its normal vector n. The angle θ made by n and the z axis, and the angle φ made by the projection of n onto the x-y plane and the x axis, will be called the spherical coordinates of n, (*Figure 9*). With the help of these spherical coordinates (φ,θ) the Cartesian coordinates of n in O.xyz are given as:

$$n_x = \sin\theta\cos\varphi \qquad n_y = \sin\theta\sin\varphi \qquad n_z = \cos\theta \tag{13}$$

Introducing into Equation (2) the stress tensor from Equation (12), and the components of the unit vector n from Equation (13), the normal stress N acting at any moment on the plane Δ is obtained:

$$\begin{aligned} N(t) = &\left[\Sigma_{xx,a}\sin\left(\frac{2\pi t}{P}\right) + \Sigma_{xx,m}\right]\cos^2\varphi\sin^2\theta \\ &+\left[\Sigma_{xy,a}\sin\left(\frac{2\pi t}{P} - \delta\right) + \Sigma_{xy,m}\right]\sin 2\varphi\sin^2\theta \end{aligned} \tag{14}$$

By inspection of the right hand side of Equation (14), one can understand that the mean value N_m corresponds to the sum of the time independent terms:

$$N_m = \sin^2\theta(\Sigma_{xx,m}\cos^2\varphi + \Sigma_{xy,m}\sin 2\varphi) \tag{15}$$

Extracting N_m from $N(t)$, developing the term $\sin(2\pi t/P - \delta)$, appearing in Equation (14) and after some manipulations the amplitude N_a is obtained:

$$N_a = \sin^2\theta|\cos\varphi|\sqrt{\Sigma_{xx,a}^2\cos^2\varphi + 4\Sigma_{xy,a}^2\sin^2\varphi + 2\Sigma_{xx,a}\Sigma_{xy,a}\sin(2\varphi)\cos\delta} \tag{16}$$

Clearly, N_a and N_m could also be obtained by direct application of their definitions, Equation (4), by evaluating through standard calculus the extrema of $N(t)$.

. To discuss the quantities related to the shear stress C, it is useful to introduce another frame O.nlr, where (l, r) are axes lying on Δ, defined as indicated in (*Figure 9*). The unit vectors along the l and r axes will be denoted as l and r. Their coordinates in the O.xyz frame are:

$$\begin{aligned} l_x &= -\sin\varphi & l_y &= \cos\varphi & l_z &= 0 \\ r_x &= -\cos\theta\cos\varphi & r_y &= -\cos\theta\sin\varphi & r_z &= \sin\theta \end{aligned} \tag{17}$$

Introducing Equations (12) and (13) into Equation (3) one obtains the shear stress C expressed in the frame O.xyz. However, it is more judicious to evaluate C in the frame O.nlr where only the components along l and r exist. These components are given as:

$$C_l = \underset{\sim}{l} \cdot \underset{\sim}{C} \quad \text{and} \quad C_r = \underset{\sim}{r} \cdot \underset{\sim}{C} \tag{18}$$

Introducing Equation (3) in these relationships leads to:

$$C_l = \underset{\sim}{l} \cdot \underset{\sim}{\Sigma} \cdot \underset{\sim}{n} \qquad C_r = \underset{\sim}{r} \cdot \underset{\sim}{\Sigma} \cdot \underset{\sim}{n} \tag{19}$$

where the fact that n is orthogonal to both l and r (i.e. $n \cdot l = n \cdot r = 0$), is taken into account. Combining Equation (19) with Equations (12), (13) and (17) one obtains:

$$\begin{aligned} C_l(t) &= -\frac{1}{2}\left[\Sigma_{xx,a} sin\left(\frac{2\pi t}{P}\right) + \Sigma_{xx,m}\right] sin\theta \; sin2\varphi \\ &\quad + \left[\Sigma_{xy,a} sin\left(\frac{2\pi t}{P} - \delta\right) + \Sigma_{xy,m}\right] sin\theta \, cos2\varphi \\ C_r(t) &= -\frac{1}{2}\left[\Sigma_{xx,a} sin\left(\frac{2\pi t}{P}\right) + \Sigma_{xx,m}\right] sin2\theta \; cos^2\varphi \\ &\quad -\frac{1}{2}\left[\Sigma_{xy,a} sin\left(\frac{2\pi t}{P} - \delta\right) + \Sigma_{xy,m}\right] sin2\theta \, sin2\varphi \end{aligned} \tag{20}$$

Developing the term $sin(2\pi t/P - \delta)$ in the above relations and rearranging terms through elementary but lengthy algebraic manipulations, lead to the formulae:

$$\begin{aligned} C_l(t) &= f \, sin\left(\frac{2\pi}{P} t\right) + g \, cos\left(\frac{2\pi}{P} t\right) \\ &\quad + \left(-\frac{\Sigma_{xx,m}}{2} sin2\varphi + \Sigma_{xy,m} cos2\varphi\right) sin\theta \\ C_r(t) &= p \, sin\left(\frac{2\pi}{P} t\right) + q \, cos\left(\frac{2\pi}{P} t\right) \\ &\quad + \left(-\frac{\Sigma_{xx,m}}{2} cos^2\varphi - \frac{\Sigma_{xy,m}}{2} sin2\varphi\right) sin2\theta \end{aligned} \tag{21}$$

where f, g, p and q are auxiliary functions:

$$\begin{aligned} f &= sin\theta\left(-\frac{\Sigma_{xx,a}}{2} sin2\varphi + \Sigma_{xy,a} cos2\varphi \, cos\delta\right) \qquad g = -\Sigma_{xy,a} sin\theta \, cos2\varphi \, sin\delta \\ p &= -\frac{1}{2} sin2\theta(\Sigma_{xx,a} cos^2\varphi + \Sigma_{xy,a} sin2\varphi \, cos\delta) \qquad q = \frac{1}{2}\Sigma_{xy,a} sin2\theta \, sin2\varphi \, sin\delta \end{aligned} \tag{22}$$

Equations (21) are the parametric equations of the curve Ψ'. They describe an ellipse in

the frame O.lr. Therefore, in out-of-phase bending and torsion, the path Ψ' described by the vector $\underset{\sim}{C}$ on Δ is an elliptic path, (*Figure 10)*.

By inspecting Equations (21) it is easy to understand that this elliptic path Ψ is centred at the point $C_{l,m}$, $C_{r,m}$) corresponding to the time independent terms of the right hand sides of these relationships, i.e.:

$$C_{l,m} = \left(-\frac{\Sigma_{xx,m}}{2}\sin 2\varphi + \Sigma_{xy,m}\cos 2\varphi\right)\sin\theta$$
$$C_{r,m} = \left(-\frac{\Sigma_{xx,m}}{2}\cos^2\varphi - \frac{\Sigma_{xy,m}}{2}\sin 2\varphi\right)\sin 2\theta \qquad (23)$$

The semi-axes of this ellipse Ψ are given by:

$$a, b = \sqrt{\frac{f^2+g^2+p^2+q^2}{2} \pm \sqrt{\left(\frac{f^2+g^2+p^2+q^2}{2}\right)^2 - (fq-gp)^2}} \qquad (24)$$

The sign (+) corresponds to the major semi-axis denoted as a, and the sign (-) to the minor semi-axis denoted as b. Obviously a and b are functions of (φ, θ).

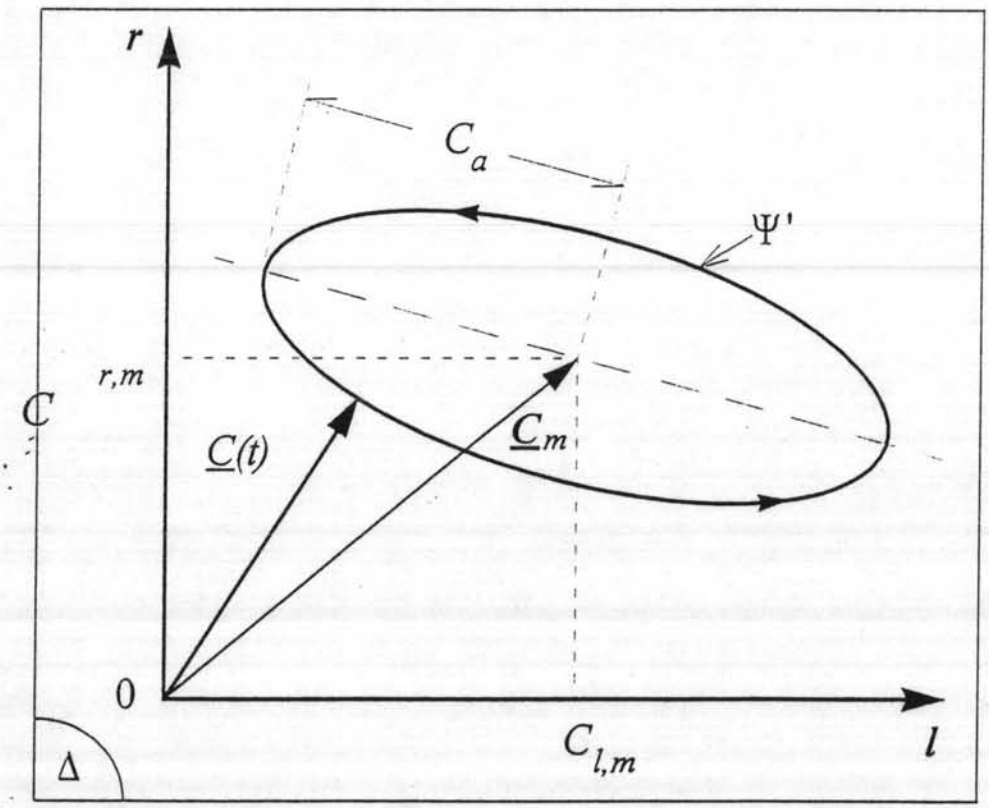

Figure 10 .Elliptic path Ψ' described on a plane Δ by the shear stress vector $\underset{\sim}{C}$ during a synchronous sinusoidal *out-of-phase* bending and torsion loading.

Clearly, the minimum circumscribed circle to the ellipse Ψ is centred at the point $C_{l,m}, C_{r,m}$) which is its centre of symmetry. The radius of this circle is equal to the major semi-axis a. Hence, the amplitude of the shear stress C_a, and the mean value C_m are given as:

$$C_a = \sqrt{\frac{f^2+g^2+p^2+q^2}{2} + \sqrt{\left(\frac{f^2+g^2+p^2+q^2}{2}\right)^2 - (fq-gp)^2}} \tag{25}$$

$$C_m = \sqrt{C_{l,m}^2 + C_{r,m}^2} \tag{26}$$

The above formulae will facilitate the application in bending and torsion of any fatigue criterion of the *critical plane* type.

Quantities related to the stress invariants

Hydrostatic Stress

The stress tensor can be split in its deviatoric and spherical parts as:

$$\underset{\sim}{\Sigma} = \underset{\sim}{S} + \frac{1}{3} tr(\underset{\sim}{\Sigma}) \underset{\sim}{I} \tag{27}$$

where I is the second order unit tensor, $tr(\Sigma)$ is the first invariant of the stress tensor equal to $tr(\underset{\sim}{\Sigma}) = (\Sigma_{xx} + \Sigma_{yy} + \Sigma_{zz})$ and $\underset{\sim}{S}$ is the stress deviator:

$$\underset{\sim}{S} = \underset{\sim}{\Sigma} - \frac{1}{3} tr(\underset{\sim}{\Sigma}) \underset{\sim}{I} \Rightarrow \underset{\sim}{S} = \begin{bmatrix} \frac{2\Sigma_{xx} - \Sigma_{yy} - \Sigma_{zz}}{3} & \Sigma_{xy} & \Sigma_{xz} \\ \Sigma_{yx} & \frac{2\Sigma_{yy} - \Sigma_{xx} - \Sigma_{zz}}{3} & \Sigma_{yz} \\ \Sigma_{zx} & \Sigma_{zy} & \frac{2\Sigma_{zz} - \Sigma_{xx} - \Sigma_{yy}}{3} \end{bmatrix} \tag{28}$$

The hydrostatic stress denoted as Σ_H, is a stress quantity frequently arising in the formulation of fatigue criteria:

$$\Sigma_H = \frac{1}{3} tr(\underset{\sim}{\Sigma}) \Rightarrow \Sigma_H(t) = \frac{1}{3} [\Sigma_{xx}(t) + \Sigma_{yy}(t) + \Sigma_{zz}(t)] \tag{29}$$

For a cyclic loading, $\Sigma_H(t)$ is a scalar periodic function of time with period P. One can easily define the hydrostatic stress amplitude $\Sigma_{H,a}$ and mean value $\Sigma_{H,m}$:

$$\Sigma_{H,a} = \frac{1}{2}\left\{ \max_{t \in P} \frac{tr(\underset{\sim}{\Sigma}(t))}{3} - \min_{t \in P} \frac{tr(\underset{\sim}{\Sigma}(t))}{3} \right\} \tag{30}$$

$$\Sigma_{H,m} = \frac{1}{2}\left\{ \max_{t\in P} \frac{tr(\underset{\sim}{\Sigma}(t))}{3} + \min_{t\in P} \frac{tr(\underset{\sim}{\Sigma}(t))}{3} \right\} \tag{31}$$

Clearly, the maximum value of the hydrostatic stress $\Sigma_{H,max}$ is equal to:

$$\Sigma_{H,max} = \Sigma_{H,a} + \Sigma_{H,m} \tag{32}$$

Second Invariant of Stress Deviator

The square root of the second invariant of the stress deviator, denoted as $\sqrt{J_2}$, is also a quantity of interest. It is defined as:

$$\sqrt{J_2} = \sqrt{\frac{1}{2}\underset{\sim}{S}\cdot\underset{\sim}{S}} \tag{33}$$

The definition of its amplitude and mean value is a quite complicated exercise. To facilitate our task the following transformation rules will be introduced:

$$S_1 = \frac{\sqrt{3}}{2}S_{xx} \qquad S_2 = \frac{1}{2}(S_{yy} - S_{zz}) \qquad S_3 = S_{xy} \qquad S_4 = S_{xz} \qquad S_5 = S_{yz} \tag{34}$$

With the above rules the stress deviator tensor is mapped onto the vector $\underset{\sim}{S}$ of a 5-dimensional Euclidian space E_5. The following equality holds:

$$\sqrt{J_2} = \sqrt{(S_1^2 + S_2^2 + S_3^2 + S_4^2 + S_5^2)} \tag{35}$$

Therefore, the length of the vector S, Equation (34), in E_5, is equal to the square root of the second invariant of the stress deviator. Thus, a vector S obtained through the transformation, Equation (34), fully represents the deviatoric stress state. During a periodic loading the tip of the vector S describes in E_5 a closed curve Φ'. The usual definition of the amplitude of $\sqrt{J_2}$, denoted as $\sqrt{J_{2,a}}$, is that it is equal to half the longest chord of Φ' (Lemaitre and Chaboche [3], Fuchs and Stephens [8]). Clearly, this definition is obtained by analogy with the previously examined Longest Chord proposal for the definition of C_a. As in that case, the definition of $\sqrt{J_{2,a}}$ through the longest chord of Φ', leads to ambiguous results because of the non-uniqueness of the longest chord, which in turn implies the non-uniqueness of the mean value $\sqrt{J_{2,m}}$. The following new definition is exempted from errors. To define $\sqrt{J_{2,a}}$ one has first to construct the (unique) minimum 5-dimensional hypersphere circumscribed to the curve Φ'. The length of the vector $\underset{\sim}{S}_m$ that points to the centre of this hypersphere is equal to the mean value $\sqrt{J_{2,m}}$, whereas $\sqrt{J_{2,a}}$ is equal to the radius of this hypersphere. The centre $\underset{\sim}{S}_m$ can be find by solving the following min-max problem:

$$\underset{\sim}{S}_m : \quad \min_{\underset{\sim}{S}'} \left\{ \max_{t \in P} \left\| \underset{\sim}{S}(t) - \underset{\sim}{S}' \right\| \right\} \tag{36}$$

The geometrical explanation of the above problem is similar to that provided previously, when dealing with the shear stress C, with the difference that here our stress path is not described in a 2-dimensional plane, but in a 5-dimensional space. The complete algorithm for constructing the minimum circumscribed hypersphere in a curve embedded in a n-dimensional Euclidian space is based on a theorem established by Papadopoulos [5] and it is merely an extension of the theorem provided before for a 2-dimensional Euclidian space (i.e. material plane Δ onto which the shear stress vector describes a closed curve Ψ'). The complete discussion concerning a curve of a n-dimensional Euclidian space is beyond the scope of the present work. However, the stress state with which we usually have to deal in fatigue is a plane stress state because the fatigue cracks frequently appear in the free surface of a specimen or a component. Then the stress state is given as:

$$\underset{\sim}{\Sigma} = \begin{bmatrix} \Sigma_{xx} & \Sigma_{xy} & 0 \\ \Sigma_{yx} & \Sigma_{yy} & 0 \\ 0 & 0 & 0 \end{bmatrix} \tag{37}$$

The stress deviator is:

$$\underset{\sim}{S} = \begin{bmatrix} \dfrac{2\Sigma_{xx} - \Sigma_{yy}}{3} & \Sigma_{xy} & 0 \\ \Sigma_{yx} & \dfrac{2\Sigma_{yy} - \Sigma_{xx}}{3} & 0 \\ 0 & 0 & -\dfrac{\Sigma_{xx} + \Sigma_{yy}}{3} \end{bmatrix} \tag{38}$$

Applying the transformation rules Equation (34) one obtains:

$$S_1 = \frac{2\Sigma_{xx} - \Sigma_{yy}}{2\sqrt{3}} \qquad S_2 = \frac{\Sigma_{yy}}{2} \qquad S_3 = \Sigma_{xy} \tag{39}$$

the remaining two components of the 5-dimensional vector, Equation (34), being equal to zero. Therefore, in this common case one deals with a curve Φ' described by the tip of the vector of Equation (39) in a 3-dimensional Euclidian space. For this case the minimum circumscribed sphere to a polytope P of m vertices, that approximates the curve Φ', is provided by the following theorem.

Theorem

The minimum circumscribed sphere to a polytope P of E_3 is: or one of the spheres drawn with diameter a line segment joining any two vertices of P, or one of the spheres a great circle of which is a circumcircle to a triangle generated from every three vertices of P or one of the circumspheres of all the tetrahedra generated from every four vertices of P.

The corresponding algorithm is similar to the one concerning the shear stress amplitude with the difference that here the combinations of the m vertices of P that should be taken into account are: the combinations of m taken two at a time (i.e. segments), the combinations of m taken three at a time (i.e. triangles) and the combinations of m taken four at a time (i.e. tetrahedra). Fortunately, if the curve Φ' possesses a centre of symmetry, the solution of the min-max problem, Equation (36), is readily available, as the centre of symmetry is also the centre of the minimum circumscribed hypersphere to Φ'. Once $\underset{\sim}{S}_m$ has been found, $\sqrt{J_{2,a}}$ is obtained by the relationship:

$$\sqrt{J_{2,a}} = \max_{t \in P} \left\| \underset{\sim}{S}(t) - \underset{\sim}{S}_m \right\| \tag{40}$$

Examples

Application in out-of-phase bending and torsion

Let us see now how these apparently difficult definitions are translated in the case of out-of-phase bending and torsion, Equation (12). The non-vanishing components of the stress deviator, Equation (28), are:

$$S_{xx} = \frac{2\Sigma_{xx}}{3} \qquad S_{yy} = -\frac{\Sigma_{xx}}{3} \qquad S_{zz} = -\frac{\Sigma_{xx}}{3} \qquad S_{xy} = S_{yx} = \Sigma_{xy} \tag{41}$$

Applying the transformation rules, Equation (34), one finds:

$$\begin{aligned} S_1 = \frac{\Sigma_{xx}}{\sqrt{3}} \Rightarrow S_1 &= \frac{\Sigma_{xx,x}}{\sqrt{3}} sin\left(\frac{2\pi t}{P}\right) + \frac{\Sigma_{xx,m}}{\sqrt{3}} \\ S_3 = \Sigma_{xy} \Rightarrow S_3 &= \Sigma_{xy,a} sin\left(\frac{2\pi t}{P} - \delta\right) + \Sigma_{xy,m} \end{aligned} \tag{42}$$

the other three components of the vector $\tilde{S}$ being equal to zero. Therefore, the stress deviator with four non-vanishing components, Equation (41), is fully described by only two components S_1 and S_3 in the transformed space. Accordingly, in this case the E_5 space reduces to a familiar bidimensional plane and the much sought-after minimum circumscribed hypersphere to Φ', degrades to a circle. The components S_1 and S_3 are the parametric equations of the curve Φ', which turns out to be an ellipse. By inspection of Equation (42) one easily concludes that the centre of this ellipse (and of

its minimum circumscribed circle), is the point:

$$S_1 = \Sigma_{xx,m}/\sqrt{3} \qquad S_3 = \Sigma_{xy,m} \tag{43}$$

Therefore, the mean value $\sqrt{J_{2,m}}$ is given as:

$$\sqrt{J_{2,m}} = \sqrt{S_{1,m}^2 + S_{3,m}^2} \Rightarrow \sqrt{J_{2,m}} = \sqrt{\frac{\Sigma_{xx,m}^2}{3} + \Sigma_{xy,m}^2} \tag{44}$$

The amplitude of the square root of J_2 is equal to the major semi-axis of this ellipse:

$$\sqrt{J_{2,a}} = \frac{1}{\sqrt{2}}\sqrt{\left(\frac{\Sigma_{xx,a}^2}{3} + \Sigma_{xy,a}^2\right) + \sqrt{\left(\frac{\Sigma_{xx,a}^2}{3} + \Sigma_{xy,a}^2\right)^2 - \frac{4}{3}\Sigma_{xx,a}^2\Sigma_{xy,a}^2(sin\delta)^2}} \tag{45}$$

Finding the amplitude and mean value of the hydrostatic stress is a trivial problem as in bending and torsion $\Sigma_H = \Sigma_{xx}/3$. One has:

$$\Sigma_{H,a} = \frac{\Sigma_{xx,a}}{3} \qquad \Sigma_{H,m} = \frac{\Sigma_{xx,m}}{3} \qquad \text{and} \qquad \Sigma_{H,max} = \frac{\Sigma_{xx,a} + \Sigma_{xx,m}}{3} \tag{46}$$

USUAL FATIGUE CRITERIA

In discussing the various criteria presented in this section, two firmly established experimental facts will be taken into consideration. They are:

-The independence of the fatigue limit in cyclic torsion with respect to a superimposed mean (static) torsion, as far as yielding of the specimen is not reached, (*Figure 11)*. This is usually the case in high-cycle fatigue.

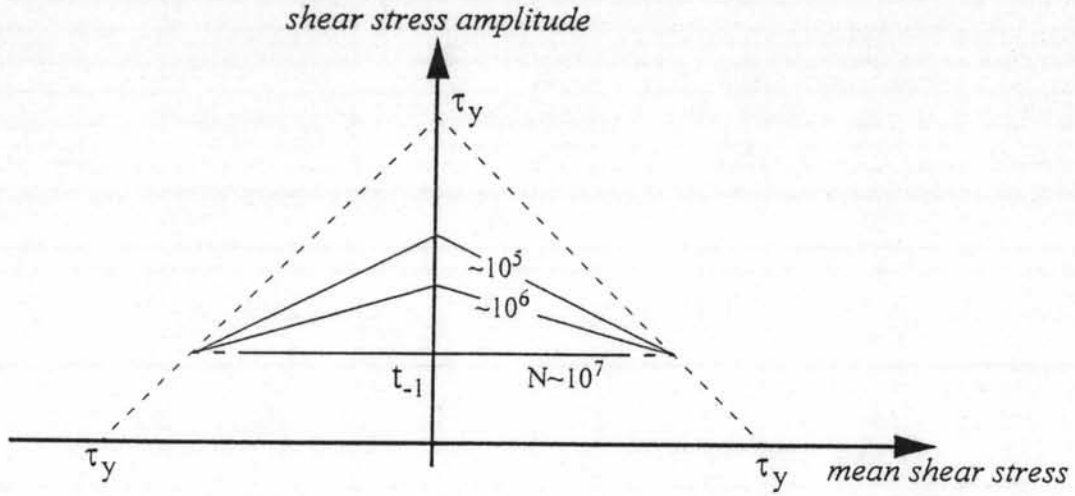

Figure 11 . Uniqueness of the fatigue limit in torsion

The amplitude of the shear stress, that can be sustained by a specimen submitted to torsion for a very high (theoretically infinite) number of cycles, is unique. This uniqueness of the fatigue limit in torsion is a well-established experimental fact, clearly demonstrated by the compilation presented by Sines, [9]. However, it is reminded that this result does not hold for finite life torsion tests. There, the presence of a mean torsion usually reduces the shear stress amplitude that can be sustained for a precise number of load cycles, (*Figure 11)*.

- The fatigue limit in bending strongly depends on a superimposed mean (static) normal stress. A tensile mean normal stress reduces the fatigue limit, whereas a compressive mean stress leads to a net increase, (*Figure 12)*.

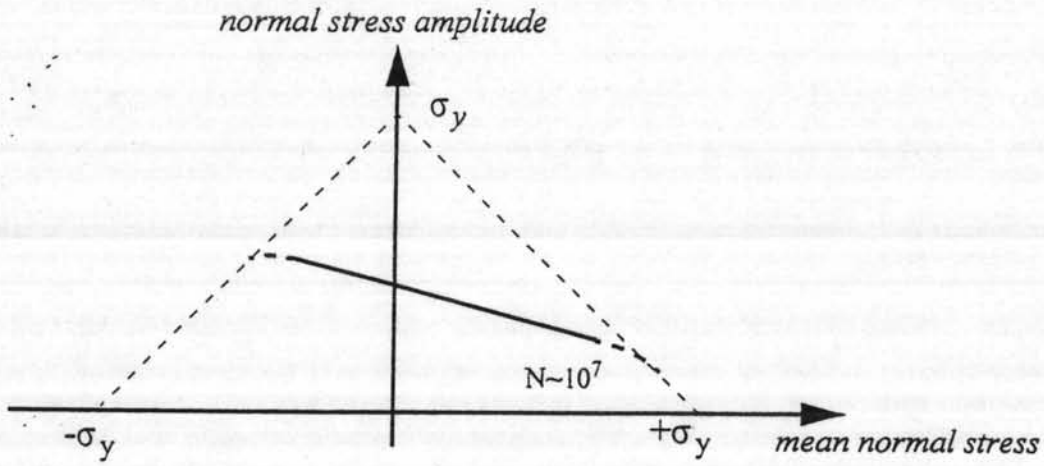

Figure 12 . Influence of a mean normal stress on the fatigue limit in tension-compression (or bending)

This dependence can be accurately described by a linear relationship as the compilations of many experimental results presented in Lemaitre and Chaboche [3] and Sines [9] have shown. Of course the above experimental finding holds in the elastic regime, (*Figure 12*).

Critical plane approaches

The ingredients of the critical plane criteria are the normal and shear stresses acting on a material plane Δ. The various proposed formulae are different, but the process to follow is merely the same. One must firstly, found the critical plane and secondly, check if the criterion is satisfied on this plane. If the criterion is not satisfied, then a fatigue crack may appear on the critical plane. Therefore, the orientation of the initiated crack coincides with the orientation of the critical plane.

The Findley criterion

The Findley criterion [10] corresponds to the limitation of the linear combination of C_a and N_{max} acting on the critical plane. This plane is defined by the spherical coordinates (φ^*,θ^*), of the unit vector n^* normal to the critical plane. Following Findley the couple (φ^*,θ^*) is determined by:

$$(\varphi^*,\theta^*): \quad \max_{(\varphi,\theta)} \{ C_a(\varphi,\theta) + \kappa N_{max}(\varphi,\theta) \} \tag{47}$$

Once the couple (φ^*,θ^*) has been found, the criterion to be satisfied is written as:

$$C_a(\varphi^*,\theta^*) + \kappa N_{max}(\varphi^*,\theta^*) \leq \lambda \tag{48}$$

where κ and λ are material parameters. Application of the above procedure in cyclic torsion with a mean shear stress (i.e. $\Sigma_{xy} = \Sigma_{xy,a} sin(2\pi t/P) + \Sigma_{xy,m}$), conducts to:

$$\Sigma_{xy,a} = \sqrt{\lambda^2 - \kappa^2 (\Sigma_{xy,a} + \Sigma_{xy,m})^2} \tag{49}$$

This means that the Findley criterion incorrectly predicts a dependence of the torsion fatigue limit with respect to a superimposed mean torsion. This criterion has been widely discussed in the past. This is the main reason to have presented it here. However, in view of the incorrect inequality, Equation (49), the Findley criterion will not be further considered in the present work.

The Matake criterion

The criterion of Matake [11] appears also as the limitation of the linear combination of C_a and N_{max} acting on the critical plane. However, the critical plane according to Matake is the plane on which the shear stress amplitude reaches its maximum:

$$(\varphi^*,\theta^*): \quad \max_{(\varphi,\theta)} \{ C_a(\varphi,\theta) \} \tag{50}$$

after which the criterion is written as the Findley criterion:

$$C_a(\varphi^*,\theta^*) + \kappa N_{max}(\varphi^*,\theta^*) \leq \lambda \qquad (51)$$

where κ and λ are material parameters. The same letters were assigned to the parameters of the Findley criterion. However, it must be understood that κ and λ take different values for each criterion. This remark holds also for the other examined criteria. The parameters κ and λ of the Matake criterion are obtained applying Equation (51), in fully reversed torsion (i.e. $C_a(\varphi^*,\theta^*)=t_{-1}$, $N_{max}(\varphi^*,\theta^*)=0$), and fully reversed bending (i.e. $C_a(\varphi^*,\theta^*)= f_{-1}/2$, $N_{max}(\varphi^*,\theta^*)= f_{-1}/2$). One obtains:

$$\kappa = (2t_{-1}/f_{-1}) - 1 \qquad \lambda = t_{-1} \qquad (52)$$

where t_{-1} and f_{-1} are the fatigue limits in fully reversed torsion and bending respectively. This criterion correctly predicts the uniqueness of the torsion fatigue limit. Moreover, it implies a linear dependence of the bending limit upon a superimposed static normal stress. The present criterion is the most classical among the critical plane approaches. Although presented here under the label 'Matake criterion' it has been studied by many other authors. The related references can be found in Papadopoulos [1]. This criterion is applied in the collected out-of-phase bending and torsion test data. The determination of the critical plane, Equation (50), is performed numerically, after what Equation (51) is applied with the values of C_a and $N_{max}=N_a+N_m$ given by Equations (25) and (15)-(16) respectively.

The Robert criterion

This author [12] proposes to separate the effects of the static part N_m and the fluctuating part $N(t)-N_m$ of the normal stress N, acting on the critical plane. Furthermore, the concept of the shear stress amplitude C_a is abandoned in the profit of the quantity $\left\| \underset{\sim}{C}(t) - \underset{\sim}{C}_m \right\|$ which directly resorts to the minimum circumscribed circle to the curve $\tilde{\Psi}$' described by C on a plane Δ. The procedures of finding the critical plane and controlling if the criterion is satisfied, are both compacted in the following relationship:

$$\max_{\varphi,\theta,t} \left\{ \left\| \underset{\sim}{C}(\varphi,\theta,t) - \underset{\sim}{C}_m(\varphi,\theta) \right\| + \kappa \left[N(\varphi,\theta,t) - N_m(\varphi,\theta) \right] + \mu N_m(\varphi,\theta) \right\} \leq \lambda \qquad (53)$$

where κ, λ and μ are material parameters which in principle can be obtained from three tests such as torsion t_{-1}, fully reversed bending f_{-1} and repeated (i.e. zero to tension) bending f_0. Although this criterion appears appealing, it suffers from the same inconsistency as the Findley proposal, that is it (incorrectly) predicts a detrimental influence of a static shear stress on the torsion fatigue limit. Indeed, application of the above procedure in cyclic torsion with a mean shear stress (i.e. $\Sigma_{xy} = \Sigma_{xy,a} sin(2\pi t/P) + \Sigma_{xy,m}$), conducts to:

$$\sqrt{\Sigma_{xy,a}^2 + (\kappa\Sigma_{xy,a} + \mu\Sigma_{xy,m})^2} \le \lambda \tag{54}$$

Furthermore, application of this criterion needs numerical calculations even for proportional loading. To the author's opinion, a fatigue criterion useful in engineering practice must provide analytical solutions when applied in simple loading conditions, such as in-phase cyclic loading. Therefore, this approach will not be further discussed here.

The McDiarmid Criterion

The critical plane according to McDiarmid [13],[14] is the plane on which the shear stress amplitude reaches its maximum value, i.e.:

$$(\varphi^*,\theta^*): \qquad \max_{(\varphi,\theta)}\{C_a(\varphi,\theta)\} \tag{55}$$

McDiarmid employs the concept of case A and case B cracks, first introduced in metal fatigue by Brown and Miller [15]. Case A cracks propagate along the surface of the specimen, whereas case B cracks propagate inwards from the surface. Case B is more severe than case A. The McDiarmid criterion is written as:

$$C_a(\varphi^*,\theta^*) + \frac{t_{A,B}}{2\sigma_f} N_{max}(\varphi^*,\theta^*) \le t_{A,B} \tag{56}$$

where σ_f is the ultimate tensile strength of the material and the shear stress limit t_A or t_B is used depending on whether the critical plane indicates that case A or case B cracks can potentially occur, respectively. In torsion, case A cracks appear and then $t_A = t_{-1}$. Case A cracks occur also under combined bending and torsion. This means that the unit vector n^* normal to the critical plane, belongs to the plane tangent to the surface of the specimen, which implies that $\theta^* = \pm\pi/2$, (*Figure 9*). Therefore, for bending and torsion the criterion becomes:

$$C_a\left(\varphi^*, \pm\frac{\pi}{2}\right) + \frac{t_{-1}}{2\sigma_f} N_{max}\left(\varphi^*, \pm\frac{\pi}{2}\right) \le t_{-1} \tag{57}$$

This criterion correctly reproduces the uniqueness of the fatigue limit in torsion. Furthermore, it implies a linear dependence of the bending limit upon a superimposed static normal stress. Equation (57), is applied in the available out-of-phase bending and torsion test data, with the help of Equations (15), (16) and (25). The critical plane is determined numerically.

The Dietmann criterion

Dietmann [16] uses the concept of octahedral shear and normal stresses, in the formulation of his criterion. The latest version of this criterion presented in Häfele and Diet-

mann [17] will be discussed here. The octahedral stresses are the stresses acting on the plane which is equally inclined to the principal directions of the stress tensor (i.e. octahedral plane). For a proportional loading the frame O.123, defined by the principal stress directions, is fixed. Therefore, in this case the octahedral plane does not move with respect to the specimen. However, under out-of-phase loading the principal stress directions (and therefore the octahedral plane) move with respect to the material. For out-of-phase bending and torsion the z axis perpendicular to the free surface of the specimen always coincides with the principal axis 3. Then the principal frame O.123 rotates around the z axis. Therefore, the unit vector n normal to the octahedral plane makes a constant angle with the z axis equal to $\theta = arcos(1/\sqrt{3})$. The position of O.123 at any moment of the cyclic loading is fully described by the angle γ that makes the (moving) axis 1 with the x axis attached to the specimen. The projection of n on the 1-2 plane makes with the axis 1 a constant angle of $\pi/4$ and therefore an angle of $(\pi/4)+\gamma$ with the x axis. In conclusion, the spherical coordinates φ and θ of the unit vector normal to the octahedral plane are given by:

$$\varphi = (\pi/4)+\gamma \qquad \theta = arcos(1/\sqrt{3}) \tag{58}$$

In the Dietmann approach the amplitude of the octahedral shear stress, denoted as $C_{oct,a}$, is firstly evaluated. For out-of-phase bending and torsion $C_{oct,a}$ can be obtained by Equation (25), where the auxiliary functions f, g, p and q, Equation (22), must be evaluated beforehand for the values of φ and θ given by Equation (58). Therefore, $C_{oct,a}$ is a function of the angle γ. An allowable octahedral stress amplitude, denoted as $C_{oct,ALL}$, is also introduced by Dietmann. The procedure of building this allowable stress is too lengthy. Therefore, only the final formula will be given here:

$$C_{oct,ALL} = \frac{f_{-1}}{\sqrt{6}} \sqrt{1 - \frac{2N_{oct,m}}{\sigma_f(1-sin2\gamma)}} \sqrt{\frac{1}{3}(1-sin2\gamma)^2 + cos^2 2\gamma} \tag{59}$$

where $N_{oct,m}$ is the mean value of the normal stress acting on the octahedral plane. For out-of-phase bending and torsion $N_{oct,m}$ can be obtained from Equation (15) upon introducing the φ and θ values given by Equation (58). Clearly, $C_{oct,ALL}$ is a function of γ. The critical octahedral plane according to the this approach is defined by the angle γ^* which renders minimum the ratio $C_{oct,ALL}/C_{oct,a}$, after what the criterion to be satisfied can be written as:

$$C_{oct,a}(\gamma^*) \le C_{oct,ALL}(\gamma^*) \tag{60}$$

The Dietmann approach is applied in the collected out-of-phase bending and torsion fatigue limit data.

Approaches based on the stress invariants

The ingredients of these fatigue criteria are the hydrostatic stress and the second invariant of the stress deviator. In principle, application of anyone of these criteria can establish if a fatigue crack may appear or not, under a cyclic load. However, the orientation of the potential fatigue crack is by no means specified by these criteria.

The Marin criterion

Marin [18] proposed a criterion based on the amplitude and mean value of $\sqrt{J_2}$. The general form of his criterion is:

$$\left(\frac{\sqrt{3J_{2,a}}}{f_{-1}}\right)^{\lambda} + \left(\kappa\frac{\sqrt{J_{2,m}}}{\sigma_f}\right)^{\mu} \leq 1 \tag{61}$$

but in practice Marin suggests to use the values of $\kappa = 1$ and $\lambda = \mu = 2$. Applying the criterion with these values in cyclic torsion with a superimposed mean shear stress (i.e. $\Sigma_{xy} = \Sigma_{xy,a} sin(2\pi t/P) + \Sigma_{xy,m}$), leads to the following inequality:

$$\left(\frac{\sqrt{3}\Sigma_{xy,a}}{f_{-1}}\right)^2 + \left(\frac{\Sigma_{xy,m}}{\sigma_f}\right)^2 \leq 1 \tag{62}$$

Therefore, the Marin criterion incorrectly predicts that the fatigue limit in torsion depends on a static shear stress. Furthermore, application of this criterion in cyclic bending with a mean normal stress (i.e. $\Sigma_{xx} = \Sigma_{xx,a} sin(2\pi t/P) + \Sigma_{xx,m}$) leads to the formula:

$$\left(\frac{\Sigma_{xx,a}}{f_{-1}}\right)^2 + \left(\frac{\Sigma_{xx,m}}{\sqrt{3}\sigma_f}\right)^2 \leq 1 \tag{63}$$

Clearly, the Marin criterion is not able to distinguish the effect of a tensile static stress from that of a compressive static stress, because the static stress $\Sigma_{xx,m}$ is squared in Equation (63). In spite of these obviously erroneous results, the Marin approach or some equivalent form of his criterion, is still suggested as a valid multiaxial high-cycle fatigue approach in modern books on fatigue[19]. This is the main reason to have discussed it here. However, we will not apply this criterion in the collected test data.

The Sines criterion

The criterion proposed by Sines [9] in the late fifties, is perhaps the most popular high-cycle fatigue criterion (Fuchs and Stephens [8]). This criterion is written as:

$$\sqrt{J_{2,a}} + \kappa\Sigma_{H,m} \leq \lambda \tag{64}$$

The parameters κ and λ can be obtained from two elementary tests, that is a torsion test where one has (i.e. $\sqrt{J_{2,a}}=t_{-1}$, $\Sigma_{H,m}=0$) and a repeated bending test (i.e. $\sqrt{J_{2,a}}=f_0/\sqrt{3}$, $\Sigma_{H,m}=f_0/3$). One finds:

$$\kappa = (3t_{-1}/f_0) - \sqrt{3} \qquad \lambda = t_{-1} \tag{65}$$

This criterion correctly reproduces the uniqueness of the torsion fatigue limit. Furthermore, it introduces a linear dependence of the bending limit upon a superimposed static normal stress. Application of this criterion in fully reversed bending leads to the equality $t_{-1}/f_{-1} = 1/\sqrt{3}$. Therefore, according to Sines the fatigue limits in torsion and fully reversed bending are in a constant ratio for all metals. This is in disagreement with experimental results which indicate that the ratio t_{-1}/f_{-1} varies from 0.5 for mild metals to 1 for brittle metals. Moreover, the limit f_0 is seldom available. Actually, the limit in fully reversed bending f_{-1} is more frequently available. Hence, to apply the Sines criterion, one usually resorts to the Goodmann line, from which the limit f_0 can be obtained as $f_0 = f_{-1}/(1+f_{-1}/\sigma_f)$. With this assumption the criterion becomes:

$$\sqrt{J_{2,a}} + \frac{\sqrt{3}f_{-1}}{\sigma_f}\,\Sigma_{H,m} \le t_{-1} \tag{66}$$

This form of the Sines criterion, combined with the values of $\sqrt{J_{2,a}}$, Equation (45) and $\Sigma_{H,m}$, Equation (46), is applied in the available out-of-phase bending and torsion experimental results.

The Crossland criterion

The criterion formulated by Crossland [20] differs from the Sines criterion only concerning the influence of the hydrostatic stress, which according to Crossland must appear in the fatigue formula by its maximum value:

$$\sqrt{J_{2,a}} + \kappa\Sigma_{H,max} \le \lambda \tag{67}$$

The parameters κ and λ can be easily related to the fatigue limits t_{-1} and f_{-1} . Indeed, for fully reversed torsion one has $\sqrt{J_{2,a}}=t_{-1}$, $\Sigma_{H,max}=0$ whereas for fully reversed bending $\sqrt{J_{2,a}}=f_{-1}/\sqrt{3}$ and $\Sigma_{H,max}=f_{-1}/3$. Application of the criterion, Equation (67), in these two cases provides the material parameters:

$$\kappa = (3t_{-1}/f_{-1}) - \sqrt{3} \qquad \lambda = t_{-1} \tag{68}$$

The uniqueness of the torsion fatigue limit is correctly reproduced by this criterion, which also implies a linear relationship of the bending limit with respect to a superimposed static normal stress. The criterion, Equation (67), combined with the values of

$\sqrt{J_{2,a}}$, Equation (45) and $\Sigma_{H,max}$, Equation (46), is applied in the available out-of-phase bending and torsion fatigue limit data.

The Kakuno-Kawada criterion

Kakuno and Kawada [21] suggest to separate the effects of the amplitude and mean value of the hydrostatic stress:

$$\sqrt{J_{2,a}} + \kappa\Sigma_{H,a} + \lambda\Sigma_{H,m} \leq \mu \tag{69}$$

The identification of the parameters of the criterion needs the knowledge of three uniaxial fatigue limits e.g. t_{-1}, f_{-1} and f_0 :

$$\kappa = (3t_{-1}/f_{-1}) - \sqrt{3} \qquad \lambda = (3t_{-1}/f_0) - \sqrt{3} \qquad \mu = t_{-1} \tag{70}$$

This criterion has been further elaborated, especially for out-of-phase loading, by Chaudonneret [22]. However, this author uses the ambiguous definition of $\sqrt{J_{2,a}}$, based on the longest chord of the curve Φ'. As it was noticed already, the limit f_0 is seldom available. Therefore, this criterion is not applied systematically to all the collected out-of-phase bending and torsion experimental results. The performance of this approach is partly evaluated from the performance of the Crossland criterion in fully reversed tests, where these two criteria coincide.

The Deperrois criterion

Deperrois [23] proposed a criterion that is based on the representation of the loading path Φ', in the transformed deviatoric space E_5. According to the methodology of this author one must firstly, find the maximum chord of Φ' in E_5, denoted as D_5. Then one must consider the sub-space orthogonal to the direction of D_5 and project the curve Φ' onto this sub-space E_4. The longest chord, denoted as D_4, of the projection of Φ' onto E_4 has to be found next. Then the sub-space E_3 orthogonal to the directions of D_5 and D_4, has to be considered and the projection of Φ' onto E_3 must be constructed, after what the maximum chord D_3 has to be found. The procedure must be repeated until we reach the sub-space E_1. The criterion of Deperrois is then written as:

$$\frac{1}{2}\sqrt{(D_1^2 + D_2^2 + D_3^2 + D_4^2 + D_5^2)} + \kappa\,\Sigma_{H,max} \leq \lambda \tag{71}$$

In many cases, as for example in bending and torsion, the transformed deviatoric space reduces to a bidimensional plane. The application of Deperrois criterion is then simplified. One has firstly, to found the maximum chord of the plane curve Φ' (i.e. D_2) and secondly, to project Φ' onto the line perpendicular to D_2. This projection is a line segment the length of which is equal to D_1. This criterion appears appealing because it attempts to provide a detailed characterisation of the loading path in the deviatoric space. However, it contains a serious error of logic. Indeed, it has been shown in a previous section that the maximum chord of the loading path Φ' in E_5 is not unique. In the

case where, for instance, two D_5 exist, then there are also two E_4 sub-spaces and the Deperrois method falls short. Obviously, this situation may also appear in the case where Φ' is a plane curve. More than one maximum chord D_2 can exist. Let us denote as $D_2^{(i)}$ i=1,2... these maximum chords. Then a multitude of lines exist, each one perpendicular to a different maximum chord $D_2^{(i)}$, and consequently a multitude of projections of Φ' on all these lines exist, inducing the breakdown of Deperrois's approach. In the loading cases where, the maximum chord of Φ' in E_5 is unique, and additionally the maximum chords of all the projections of Φ' on the subsequent sub-spaces E_4 to E_1 are unique, the Deperrois criterion provides satisfactory results [24]. Nevertheless, because of the basic error of logic contained in the Deperrois's methodology, this criterion will not be further considered here.

Criteria based on stress averages within the elementary volume

The ingredients of these criteria are average quantities within V, of the shear and normal stresses acting on a material plane Δ. In general, these average quantities are described through a double integral extending over θ and φ, where θ and φ are the spherical coordinates of the unit vector n normal to a plane Δ. The integral over θ extends from 0 to π, and the integral over φ extends from 0 to 2π. In this way, all the possible orientations of the plane Δ inside V, are taken into consideration.

Grubisic and Simbürger proposal

These authors [2], propose to classify the metals into three categories according to the value of the t_{-1}/f_{-1} ratio. Only the proposal concerning the broader category of hard metals (i.e. $0.57 < t_{-1}/f_{-1} < 0.9$) will be discussed here. The rather complicated method of Grubisic and Simbürger can be condensed in the following formula:

$$\sqrt{\frac{15}{2}}\sqrt{\frac{1}{4\pi}\int_{\varphi=0}^{2\pi}\int_{\theta=0}^{\pi} A_n^2 \sin\theta\, d\theta\, d\varphi} \leq 1 \qquad (72)$$

The term A_n is called by these authors "effective straining" of a material plane Δ. To define A_n the following "equivalent" amplitude and mean value are introduced on Δ:

$$\begin{aligned} S_a(\varphi,\theta) &= \kappa C_a(\varphi,\theta) + \lambda N_a(\varphi,\theta) \\ S_m(\varphi,\theta) &= \kappa C_m(\varphi,\theta) + \lambda N_m(\varphi,\theta) \end{aligned} \qquad (73)$$

An allowable stress amplitude is defined with the help of the Haigh diagram, which for *proportional* loading can be written as:

$$\sigma_{ALL}(\varphi,\theta) = \frac{(f_0 - f_{-1})}{f_0} S_m(\varphi,\theta) + f_{-1} \qquad (74)$$

Finally, A_n is defined by the ratio:

$$A_n = S_a(\varphi, \theta)/\sigma_{ALL}(\varphi, \theta) \tag{75}$$

The parameters κ and λ are related to t_{-1} and f_{-1} through two cumbersome formulae reported in Grubisic and Simbürger [2]. The most spurious assumption of their work is the use of the same material parameters κ and λ to built the "equivalent" quantities S_a and S_m, Equation (73). Mainly because of this unfounded assumption, application of the Grubisic and Simbürger criterion in cyclic torsion with a mean shear stress leads to:

$$\frac{2\Sigma_{xy,a}}{f_{-1}} - \left(\frac{2}{f_{-1}} - \frac{2}{f_0}\right)|\Sigma_{xy,m}| \leq 1 \tag{76}$$

This relationship implies that the effect of a static shear on the torsion fatigue limit is merely as strong as the effect of a static normal stress on the limit in bending. This approach is not applied to the collected bending and torsion test data.

Liu and Zenner criterion

This criterion [25] can be written as:

$$\sqrt{\frac{15}{8\pi}\int_{\varphi=0}^{2\pi}\int_{\theta=0}^{\pi}[\kappa C_a^2(1+\mu C_m^2)+\lambda N_a^2(1+\nu N_m)]\sin\theta\, d\theta\, d\varphi} \leq f_{-1} \tag{77}$$

where κ, λ, μ and ν are material parameters related to four uniaxial fatigue limits through some rather complicated formulae reported in Liu and Zenner [25]. The old definitions of C_a and C_m based on the longest chord of the curve Ψ', described by $\tilde{C}$ on a plane Δ, are used by these authors. Moreover, the number of four material parameters introduced, is an obvious disadvantage of this criterion. Finally, this approach implies that the torsion fatigue limit depends on a superimposed static shear stress, which is in clear disagreement with experimental results, as it is pointed out previously in this work. Therefore, this approach is not applied to the collected bending and torsion test data.

APPLICATIONS AND DISCUSSION

Twelve usual multiaxial high-cycle fatigue criteria have been carefully though briefly examined in this work. Only five criteria, namely the criteria of Crossland, Sines, Matake, McDiarmid and Dietmann, have been selected for application against the out-of-phase bending and torsion experimental results found in the relevant literature. The reasons of excluding from the applications, some of the criteria examined, are explained in the sections where the various criteria have been presented. The collected out-of-phase bending and torsion experimental results are reported in Table . They come from various sources. Here, they are retrieved from the following publications: Zenner et al. [26], McDiarmid [27] and Froustey and Lasserre [28]. Experimental results for four different materials are presented in Table . The first four columns of this table contain, for each test, the amplitude and mean value of the normal stress due to bending and of the shear stress due to torsion, respectively. In the fifth column the phase difference between these two stresses is reported. The stress values presented correspond to the limiting state of non-fracture of the specimen for a number of load cycles of the order of one million. The next five columns of Table (i.e. columns 6 to 10) are dedicated to the five fatigue criteria maintained for application against the available test data, which are the criteria of Crossland, Sines, Matake, McDiarmid and Dietmann. The order of presentation follows the chronological order of publication of these works. The values appearing in these columns are the values that achieves the error index, denoted as I, which measures the deviation of the prediction of the criterion with respect to the experimentally observed values. The definition of I is the following. All the five criteria have been presented in the form of an inequality in the previous sections. If for a particular experiment, after substitution of the experimental values in the corresponding formula, the left and right hand sides of the inequality expressing the criterion are equal, then the prediction exactly agrees with the test result. If the left and right hand sides differ, then the prediction deviates from the experimental value. Therefore, the error index I, is defined to measure the relative difference between the left and right hand sides of the inequality expressing each criterion, that is:

$$I = \frac{left\ hand\ side - right\ hand\ side}{right\ hand\ side}\ (\%) \qquad (78)$$

It can be seen from columns 6 to 10 of Table that, this error index achieves for all the criteria values as high as ±30% for some experiments.

It is interesting to examine the algebraic value of the error index I, because in this way the dispersion of the predictions of each criterion can be observed. To this end (*Figure 13)* has been drawn.

Table 1. Out-of-phase bending and torsion fatigue limit data

	$\Sigma_{xx,a}$ (MPa)	$\Sigma_{xx,m}$ (MPa)	$\Sigma_{xy,a}$ (MPa)	$\Sigma_{xy,m}$ (MPa)	δ (0)	Error Index I (%)				
						Crossland	Sines	Matake	McDiarmid	Dietmann
Material: Hard Steel $f_{-1} = 313.9t_{-1} = 196.2\sigma_f = 680$Nishihara data reported in McDiarmid [27]										
1	138.1	0	167.1	0	0	-2.3	-5.6	1.0	-2.8	2.2
2	140.4	0	169.9	0	30	-4.7	-8.1	3.6	-1.2	1.8
3	145.7	0	176.3	0	60	-4.9	-8.5	8.4	1.5	0.5
4	150.2	0	181.7	0	90	-3.7	-7.4	11.8	3.7	0.3
5	245.3	0	122.65	0	0	1.5	-4.5	4.0	-2.6	3.4
6	249.7	0	124.85	0	30	-3.9	-10.0	5.2	-2.5	2.3
7	252.4	0	126.2	0	60	-12.0	-18.1	2.7	-7.4	-4.9
8	258.0	0	129.0	0	90	-17.8	-24.1	-1.4	-15.3	-14.8
9	299.1	0	62.8	0	0	0.9	-6.4	1.7	-6.3	1.4
10	304.5	0	63.9	0	90	-3.0	-10.4	-1.4	-10.3	-2.4
Material: 42CrMo4 $f_{-1} = 398t_{-1} = 260\sigma_f = 1025$Lempp data reported in Zenner [26]										
11	328.0	0	157.0	0	0	4.2	-5.4	6.8	-4.6	7.2
12	286.0	0	137.0	0	90	-28.1	-36.5	-21.6	-35.3	-25.7
13	233.0	0	224.0	0	0	7.3	0.5	10.7	2.7	13.6
14	213.0	0	205.0	0	90	-14.6	-21.2	3.8	-11.0	-11.0
15	266.0	0	128.0	128	0	-15.0	-23.1	-2.5	-18.1	-13.1
16	283.0	0	136.0	136	90	-28.9	-37.2	-6.4	-29.4	-19.0
17	333.0	0	160.0	160	180	5.9	-3.8	20.9	1.6	12.1
18	280.0	280	134.0	0	0	-2.9	4.9	19.1	-7.0	1.7
19	271.0	271	130.0	0	90	-24.0	-16.4	-9.7	-32.1	-22.4
Material: 34Cr4 $f_{-1} = 410t_{-1} = 256\sigma_f = 795$Zenner et al. [26] data										
20	314.0	0	157.0	0	0	-0.6	-6.3	2.0	-3.4	13.1
21	315.0	0	158.0	0	60	-15.8	-21.6	-1.8	-9.8	-9.0
22	316.0	0	158.0	0	90	-22.9	-28.8	-7.6	-18.4	-20.1
23	315.0	0	158.0	0	120	-15.8	-21.6	-1.8	-9.8	-9.5
24	224.0	0	224.0	0	90	-8.4	-12.5	9.3	1.6	-5.4
25	380.0	0	95.0	0	90	-7.3	-14.3	-5.1	-12.4	-6.6
26	316.0	0	158.0	158	0	0.1	-5.7	13.5	4.2	2.0
27	314.0	0	157.0	157	60	-16.2	-21.9	-0.5	-9.1	-11.8
28	315.0	0	158.0	158	90	-23.2	-28.9	1.6	-12.5	-7.0
29	279.0	279	140.0	0	0	-6.4	15.8	13.9	1.0	3.0
30	284.0	284	142.0	0	90	-25.5	-2.9	10.7	-8.8	-17.7
31	355.0	0	89.0	178	0	-6.2	-12.7	10.3	-1.3	-5.6
32	212.0	212	212.0	0	90	-9.4	7.5	24.0	9.5	-12.3
33	129.0	0	258.0	0	90	3.2	0.8	13.3	8.9	9.0
Material: 30NCD16 $f_{-1} = 660t_{-1} = 410\sigma_f = 1880$Froustey and Lasserre [28] data										
34	485.0	0	280.0	0	0	1.8	-3.4	4.7	-3.2	3.9
35	480.0	0	277.0	0	90	-27.3	-32.4	-4.1	-19.7	-23.5
36	480.0	300	277.0	0	0	3.9	10.4	19.2	2.8	8.8
37	480.0	300	277.0	0	45	-7.8	-1.3	17.8	-1.5	0.5
38	470.0	300	270.0	0	60	-14.6	-8.0	13.7	-7.1	-8.0
39	473.0	300	273.0	0	90	-25.1	-18.6	12.3	-12.9	-20.2
40	590.0	300	148.0	0	0	0.1	5.4	11.0	-5.8	8.4
41	565.0	300	141.0	0	45	-8.7	-3.2	4.0	-12.7	0.1
42	540.0	300	135.0	0	90	-15.0	-9.1	-7.4	-22.1	-12.7
43	211.0	300	365.0	0	0	-0.7	8.7	16.3	3.3	6.8

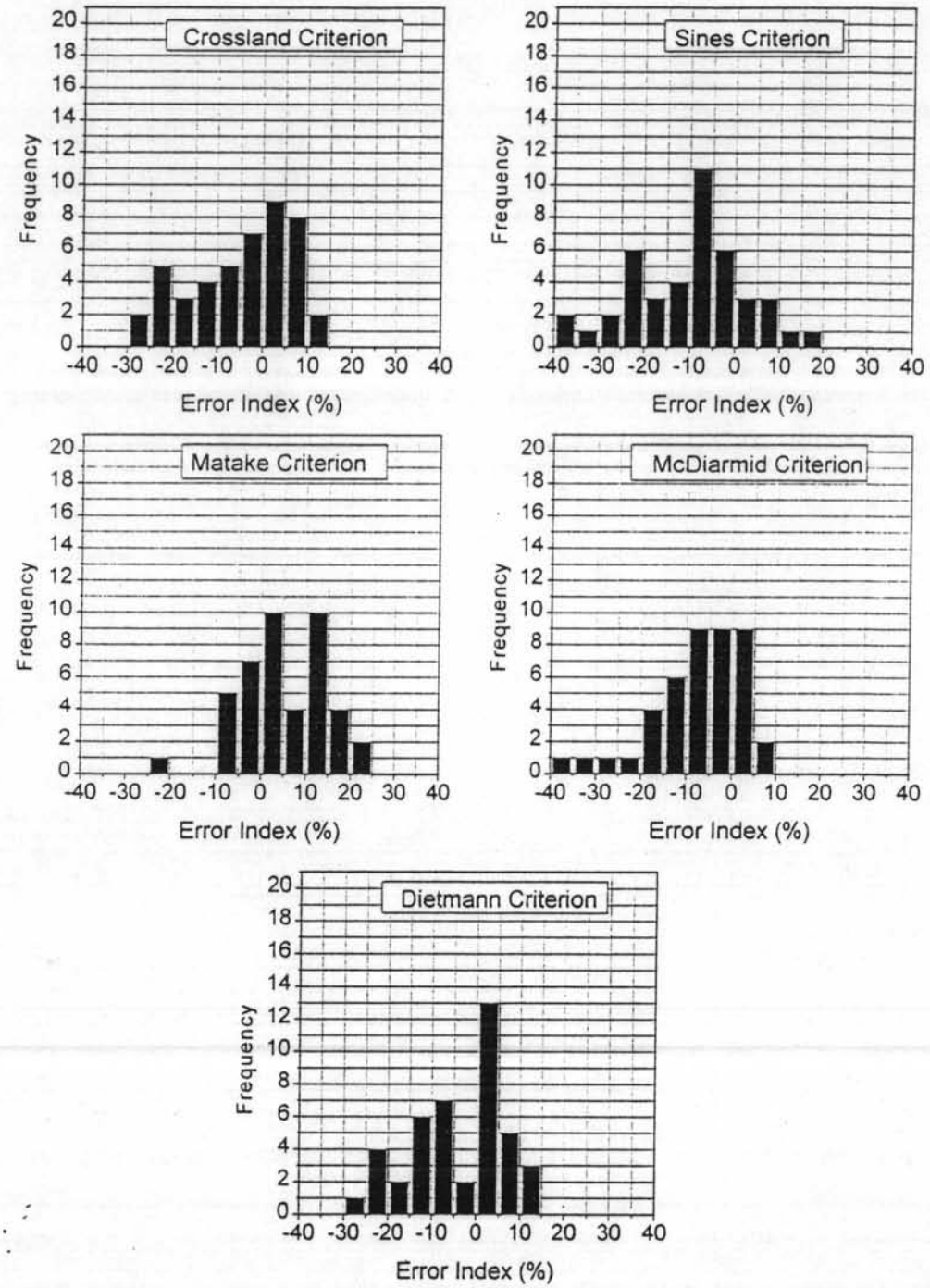

Figure 13 .Frequency histograms showing the dispersion of the relative difference between predictions and experimental values for some criteria

This figure is made up from five different graphs each one corresponding to a different criterion. These graphs show frequency histograms that have been built as follows. The abscissa is the value of the error index I. The values of I ranging from -40% to +40% have been separated in 16 classes (intervals) of equal range (i.e. 5%). Above each interval a column has been drawn with a height equal to the number of experiments

with a value of I falling in this interval. To make things clear let as examine the first of graphs of (*Figure 13)*. This graph corresponds to the Crossland criterion. Let us examine the experiments for which the error between prediction and experimental value belongs to the class from 0% to 5%. From column 6 of Table , corresponding to Crossland criterion, we can find that, out of a total of 43 experiments, there are 9 experiments for which the error index I has a value falling between 0% and 5%. Therefore, the column drawn above the interval 0%-5% has a height equal to nine. Obviously, predictions of a criterion can be considered as satisfactory, if the errors between prediction and experimental value are concentrated in the classes around 0%. Clearly this is not the case of the Crossland criterion. Indeed, the error index I attains values ranging from -30% to +15% for this criterion. Moreover, there are not more than nine experiments belonging to a single class of I values, which means that the predictions of this criterion are highly dispersed. Situation is not much better for Sines criterion. From (*Figure 13)* one can observe that the I index ranges from -40% to +20%. Predictions of this criterion also display a high dispersion. We will not insist in describing separately each one of the graphs of Matake, McDiarmid and Dietmann criteria. The corresponding histograms of (*Figure 13)* are self-explanatory. The comparative study carried out in this work clarified that none, among the criteria examined, showed good agreement with out-of-phase bending and torsion experimental results. The need of formulating a new fatigue limit criterion is then clear.

REFERENCES

1. Papadopoulos, I.V. (1987) *Fatigue polycyclique des métaux: Une nouvelle approche*. Thèse de Doctorat, Ecole Nationale des Ponts et Chaussées, Paris.

2. Grubisic, V. and Simbürger, A. (1976) Fatigue under combined out of phase multiaxial stresses. In *Proc. Int. Conf. on Fatigue Testing and Design*, pp. 27.1-27.8, Society of Environmental Engineers, London.

3. Lemaitre, J. and Chaboche, J.-L. (1990) *Mechanics of solid materials*. Cambridge University Press, Cambridge.

4. Dang Van, K. , Le Douaron, A. and Lieurade, H.P. (1984) Multiaxial fatigue limit: A new approach. In *Advances in Fracture Research, Proc. 6th Int. Conf. Fract. (I.C.F. 6)*, pp. 1879-1885, Pergamon Press, Oxford.

5. Papadopoulos, I. V. (1987) Annexe A-1: La plus petite hypersphère circonscrite à une courbe donnée, In *Fatigue polycyclique des métaux: Une nouvelle approche*. Thèse de Doctorat, Ecole Nationale des Ponts et Chaussées, Paris.

6. Lay, S. R. (1982) *Convex sets and their applications*. John Wiley & Sons, New York.

7. Dang Van, K. , Griveau, B. and Message, O. (1989) On a new multiaxial fatigue limit criterion: theory and application. In *Biaxial and Multiaxial Fatigue,* EGF 3 (editors M.W. Brown and K.J. Miller), pp.479-496, Mechanical Engineering Publications, London.

8. Fuchs, H.O. and Stephens, R.I. (1980) *Metal fatigue in engineering.* John Wiley & Sons, New York.

9. Sines, G. (1959) Behaviour of metals under complex static and alternating stresses. In *Metal Fatigue* (editors G. Sines and J.L. Waisman), pp. 145-169, McGraw Hill, New York.

10. Findley, W.N. (1959) A theory for the effect of mean stress on fatigue under combined torsion and axial load or bending. *Trans. ASME Ser B* , Vol. 81, pp. 301-306.

11. Matake, T. (1977) An explanation on fatigue limit under combined stress. *Bulletin of JSME* , Vol. 20, No. 141, pp. 257-263.

12. Robert, J.-L. (1992) *Contribution à l'étude de la fatigue multiaxiale sous sollicitations périodiques ou aléatoires.* Thèse de Doctorat, Institut National des Sciences Appliquées de Lyon, Lyon.

13. McDiarmid, D.L. (1991) A general criterion for high-cycle multiaxial fatigue failure. *Fatigue Fract. Engng Mater. Struct.*, Vol. 14, No. 4, pp. 429-453.

14. McDiarmid, D.L. (1994) A shear stress based critical-plane criterion of multiaxial fatigue failure for design and life prediction. *Fatigue Fract. Engng Mater. Struct.*, Vol. 17, No. 12, pp. 1475-1484.

15. Brown, M.W. and Miller, K.J. (1973) A theory for fatigue under multi-axial stress-strain conditions. *Proc. Inst. Mech. Engrs*, Vol. 187, pp. 745-755.

16. Deitmann, H., Bhongbhibhat, T. and Schmid, A. (1991) Multiaxial Fatigue Behaviour of steels under in-phase and out-of-phase loading, including different wave forms and frequencies. In *Fatigue Under Biaxial and Multiaxial Loading'*(editors K. Kussmaul, D.L. McDiarmid and D. Socie), ESIS 10, pp. 449-464, Mechanical Engineering Publications, London.

17. Häfele, P. and Dietmann, H. (1994) Wieterentwicklung der modifizierten oktaederschubspannungshypothese. H. *Konstruktion*, Vol. 46, pp. 51-58.

18. Marin, J. (1956) Interpretation of fatigue strengths for combined stresses. In *Proc. Int. Conf. on Fatigue of Metals*, pp.184-194, Institution of Mechanical Engineers, London.

19. Suresh, S. (1991) *Fatigue of materials*. Cambridge University Press, Cambridge.

20. Crossland, B. (1956) Effect of large hydrostatic pressures on the torsional fatigue strength of an alloy steel. In *Proc. Int. Conf. on Fatigue of Metals*, pp.138-149, Institution of Mechanical Engineers, London,

21. Kakuno, H. and Kawada, Y. (1979) A new criterion of fatigue strength of a round bar subjected to combined static and repeated bending and torsion. *Fatigue Engng Mater. Struct.*, Vol. 2, pp. 229-236.

22. Chaudonneret, M. (1993) A simple and efficient multiaxial fatigue damage model for engineering applications of macro-crack initiation. *Trans. ASME, J. Engng Mater. Tech.*, Vol. 115, pp. 373-379.

23. Deperrois, A. (1991) *Sur le calcul de limites d'endurance des aciers*. Thèse de Doctorat, Ecole Polytechnique, Paris.

24. Ballard, P., Dang Van, K., Deperrois, A. and Papadopoulos, I.V. (1995) High-cycle fatigue and finite element analysis. *Fatigue Fract. Engng Mater. Struct.*, Vol. 18, No. 3, pp. 397-411.

25. Liu, J. and Zenner, H. (1993) Berechnung der dauerschwingfestigkeit bei mehrachsinger beanspruchung. *Mat.-wiss. u. Werkstofftech.*, Vol. 24, pp. 240-249.

26. Zenner, H., Heidenreich, R. and Richter, I. Z. (1985) Dauerschwingfestigkeit bei nichtsynchroner mehrachsinger beanspruchung.. *Werkstofftech.*, Vol. 16, pp. 101-112.

27. McDiarmid, D.L. (1987) Fatigue under out-of-phase bending and torsion. *Fatigue Fract. Engng Mater. Struct.*, Vol. 9, No. 6, pp. 457-475.

28. Froustey, C. and Lasserre, (1989) S. Multiaxial fatigue endurance of 30NCD16 steel. *Int. J. Fatigue*, Vol. 11, No. 3, pp. 169-175.